

Sensitivity Analysis Report - Part I  
DRSPALL Version 1.00

Report for  
Conceptual Model Peer Review  
convening  
July 7-11, 2003

Authors:  
David Lord, SNL  
David Rudeen, GRAM, Inc.

August 2003

## Table of Contents

1	TEST OBJECTIVE.....	5
2	PROBLEM SETUP .....	5
2.1	Parameter Sampling .....	5
2.2	Code flow for sensitivity study .....	6
2.3	Output variable definitions .....	8
2.3.1	Radial variables.....	8
2.3.2	Pressure variables.....	10
2.3.3	Equivalent volumes.....	10
2.4	System specifications.....	11
3	RESULTS AND DISCUSSION – SPHERICAL GEOMETRY .....	11
3.1	First sample: Initial Repository Pressure = 8 – 15 MPa .....	11
3.1.1	Vector 020.....	13
3.1.2	Vector 007.....	16
3.2	Second sample: Initial Repository Pressure = 12 – 15 MPa.....	19
3.2.1	Vector 020, high pressure .....	20
3.2.2	Vector 007, high pressure .....	22
3.3	Scatterplots.....	24
3.3.1	Variables controlling equivalent uncompacted spall volume .....	25
3.3.2	Variables controlling tensile radius .....	27
4	RESULTS AND DISCUSSION – CYLINDRICAL GEOMETRY.....	30
4.1	Cylindrical vs. Spherical Geometry .....	30
4.2	Vector 020 cylindrical vs. spherical results .....	33
4.2.1	History variables .....	33
4.2.2	Spatial variables .....	34
5	SUMMARY .....	44
	REFERENCES .....	45
	APPENDIX DEFAULTS .....	46
	APPENDIX LHS2_DRSPALL.TRN .....	48
	APPENDIX VARIABLE GLOSSARY .....	64

## List of Figures

Figure 2-1. Code flow diagram for DRSPALL pre-processors. ....	7
Figure 2-2. Code flow diagram for DRSPALL post-processors.....	7
Figure 2-3. Radial variables in cylindrical geometry.....	9
Figure 2-4. Radial variables in spherical geometry. ....	9
Figure 2-5. Schematic of the relationship among TOTVOLEQ, CUTVOLEQ, and SPLVOLEQ. ....	11
Figure 3-1. Pressure history plot for v020. ....	14
Figure 3-2. Radius variables history plot for v020. ....	15
Figure 3-3. Equivalent volumes history plot for v020.....	16
Figure 3-4. Pressure history plot for v007. ....	17
Figure 3-5. Radius variables history plot for v007. ....	17
Figure 3-6. Velocity history plot for v007.....	18
Figure 3-7. Equivalent uncompact volume plot for v007. ....	18
Figure 3-8. Radius variables history plot for v020, high pressure case. ....	21
Figure 3-9. Velocity history plot for v020, high pressure case.....	21
Figure 3-10. Equivalent uncompact volume history plot for v020, high pressure case.....	22
Figure 3-11. Radius variables history plot for v007, high pressure case. ....	23
Figure 3-12. Velocity history plot for v007, high pressure case.....	23
Figure 3-13. Equivalent uncompact volume history plot for v007, high pressure case.....	24
Figure 3-14. Scatterplot of SPLVOLEQ vs. REPIPRES for all 60 vectors.....	25
Figure 3-15. Scatterplot of SPLVOLEQ vs. TENSLSR for all 60 vectors. ....	26
Figure 3-16. Scatterplot of SPLVOLEQ vs. SHAPEFAC*PARTDIAM for all 60 vectors...27	27
Figure 3-17. Schematic of definition of TENSRAD-CUTRAD output variable.....	27
Figure 3-18. Scatterplot of TENSRAD-CUTRAD vs. REPIPRES for all 60 vectors. ....	28
Figure 3-19. Scatterplot of TENSRAD-CUTRAD vs. TENSLSR for all 60 vectors. ....	28
Figure 3-20. Scatterplot of TENSRAD-CUTRAD vs. REPIPERM for all 60 vectors.....	29
Figure 4-1. Equivalent radius and volume for one-dimensional hemispherical and cylindrical geometries.....	31
Figure 4-2. Radial elastic stress profiles for one-dimensional hemispherical and cylindrical geometries.....	32
Figure 4-3. Bottomhole and cavity pressure histories .....36	36
Figure 4-4. Cuttings, spall and total equivalent uncompact volume histories .....37	37
Figure 4-5. Cavity, tensile and equivalent drilling radii histories.....38	38
Figure 4-6. Fluidization threshold and superficial pore velocity histories .....39	39
Figure 4-7. Pore pressure and radial elastic (total) stress profiles for entire repository domain.....	40
Figure 4-8. Radial effective and seepage stress profiles for entire repository domain.....	41
Figure 4-9. Radial effective stress profile (magnification 1).....	42
Figure 4-10. Radial effective stress profile (magnification 2).....	43

## List of Tables

Table 2-1. Summary of sampled DRSPALL input variables, including range and distribution. ....	6
Table 3.1. Results of 8-15 MPa LHS sampling. A glossary of variable names is given in Appendix VARIABLE GLOSSARY. ....	12
Table 3-2. Summary of equivalent uncompacted spall volumes (m <sup>3</sup> ) calculated for the 8-15 MPa sensitivity runs.....	13
Table 3-3. Sampled pressures for high-pressure sensitivity matrix.....	19
Table 3-4. Summary of equivalent uncompacted spall volumes (m <sup>3</sup> ) calculated for the 8-15 MPa and 12-15MPa sensitivity runs. ....	20
Table 4-1. Summary of equivalent uncompacted spall volumes (m <sup>3</sup> ) calculated for the 12-15 MPa sensitivity runs for spherical and cylindrical geometries.....	33
Table VG-1. Property Names .....	64
Table VG-2. History Variables (at a location or spatial integrated value) .....	66
TableVG- 3. Element Variables (space and time dependent).....	68

## Glossary of Acronyms

<i>Acronym</i>	<i>Definition</i>
CCA	Compliance Certification Application (1996)
DDZ	Drilling-damaged zone
DOE	U.S. Department of Energy
DRSPALL	Computer code that implements the new conceptual model for spallings
LHS	Latin Hypercube Sampling
PA	Performance Assessment
PAVT	Performance Assessment Verification Test (1997)
SNL	Sandia National Laboratories
TSPA	Total System Performance Assessment
WIPP	Waste Isolation Pilot Plant

## 1 TEST OBJECTIVE

This report documents the DRSPALL sensitivity study executed in support of the WIPP Spallings Model Conceptual Model Peer Review convened July 7-9, 2003, in Albuquerque, NM. This is Part I of a sensitivity study series that addresses the panel's requests to (i) capture the oral presentation "DRSPALL Sensitivity Study," given on July 9, 2003, in report format, and (ii) build a DRSPALL "response surface" based on sensitivities to key variables elucidated by Part I. The DRSPALL response surface for the peer review panel will be presented in the forthcoming Part II of this report. Most of the figures that appear in this report come directly from the oral presentation, "DRSPALL Sensitivity Study," presented by David Lord and David Rudeen at the peer review meeting on July 9, 2003.

The objectives of this analysis (Part I) are twofold:

1. To test the DRSPALL code stability over the entire parameter space possible in the WIPP Performance Assessment
2. To identify uncertain parameters that have the most impact on code output

Successful completion of this sensitivity analysis will provide reassurance that the model will behave appropriately and stably when run in the broad parameter space encountered in the WIPP total system performance assessment (TSPA). Moreover, this analysis will allow close inspection for proper implementation of the conceptual model by illustrating the relationships between key inputs such as pressure and tensile strength and outputs such as tensile failure radius and total spall release.

## 2 PROBLEM SETUP

This analysis focuses on the relationship between uncertain input parameters and code output, addressing what is referred to as subjective uncertainty in the Waste Isolation Pilot Plant Performance Assessment (WIPP PA) context. Uncertainties related to time of intrusion, number of previous intrusions, etc., are not addressed here. Rather, these will be handled when the code is integrated into the TSPA.

### 2.1 Parameter Sampling

Latin Hypercube Sampling (LHS) (Helton and Davis, 2002) was used to generate the sampled input parameters sets. LHS is a Monte Carlo technique that is frequently used in uncertainty and sensitivity analyses of complex models. The technique was chosen here due to : (a) conceptual simplicity and ease of implementation, (b) robust sampling over the range over the full range of variability of each sampled variable, and (c) it is the current standard for sampling uncertain parameters used in WIPP PA.

DRSPALL requires more than 40 input parameters in order to execute, with a complete list given in appendix DEFAULTS. Within this list, fifteen parameters were deemed

sufficiently uncertain and potentially important to code output that they were sampled in the sensitivity analysis described here. Two parameter samplings were run, with the only difference being that the repository gas pressure range was varied from 8-15 MPa in the first sampling, and 12-15 MPa in the second sampling. Table 2-1 shows the parameter names, ranges, and distribution type used for the first sampling. Note that the second sampling is identical except for constraining the pressure range to 12-15 MPa. The reason for running the second sampling was that most of the spall failure and thus interesting model behavior occurs only at pressures above 12 MPa, and the second sampling allowed for more output resolution in the parameter space that leads to spalling. The rationale for the endpoints of the sampled parameters is presented in the Parameter Justification Report for DRSPALL (Hansen et al., 2003). The distributions take two forms, either uniform or loguniform. In the event that the endpoints range over more than one order of magnitude, the distribution is loguniform. Relative to a uniform distribution, loguniform biases the sampling toward the low end of the range, deemed a conservative assumption in all four cases because low values of waste permeability, tensile strength, wellbore wall roughness, and drilling damaged zone (DDZ) permeability are understood to lead to higher or more likely spillings releases.

*Table 2-1. Summary of sampled DRSPALL input variables, including range and distribution.*

<i>Variable Name</i>	<i>Units</i>	<i>Distribution</i>	<i>Low</i>	<i>High</i>
Repository Gas Pressure	Pa	UNIFORM	8.00E+06	1.49E+07
Porosity of Waste	-	UNIFORM	3.50E-01	6.60E-01
Permeability of Waste	m <sup>2</sup>	LOGUNIFORM	1.70E-14	1.70E-12
Poisson's Ratio of Waste	-	UNIFORM	3.50E-01	4.30E-01
Tensile Strength of Waste	Pa	LOGUNIFORM	1.20E+05	1.70E+05
Initial Mud Density	kg/m <sup>3</sup>	UNIFORM	1.14E+03	1.38E+03
Initial Mud Viscosity	Pa*s	UNIFORM	5.00E-03	3.00E-02
Max Solids Vol Fraction in Mud	-	UNIFORM	5.90E-01	6.40E-01
Solids Viscosity Exponent	-	UNIFORM	-1.80E+00	-1.20E+00
Drill Penetration Rate	m/s	UNIFORM	2.96E-03	5.93E-03
Mud Pump Rate	m <sup>3</sup> /s	UNIFORM	1.61E-02	2.42E-02
DDZ Permeability	m <sup>2</sup>	LOGUNIFORM	1.00E-15	1.00E-13
Wall Roughness	m	LOGUNIFORM	5.00E-05	3.10E-03
Particle Shape Factor	-	UNIFORM	1.00E-01	1.00E+00
Particle Diameter	m	UNIFORM	1.00E-03	1.00E-02

## 2.2 Code flow for sensitivity study

The sensitivity study requires that a series of codes are run in order to create the input files, execute DRSPALL, and view the output. Input files are created by pre-processors, while output data are read and displayed by post-processors. The general code flow is shown in Figures 2-1 and 2-2.

The first step requires running MATSET to create a generic input file for DRSPALL. The input file to MATSET specifies all material names and default property values. The output from MATSET is a binary file that is read directly by LHS.

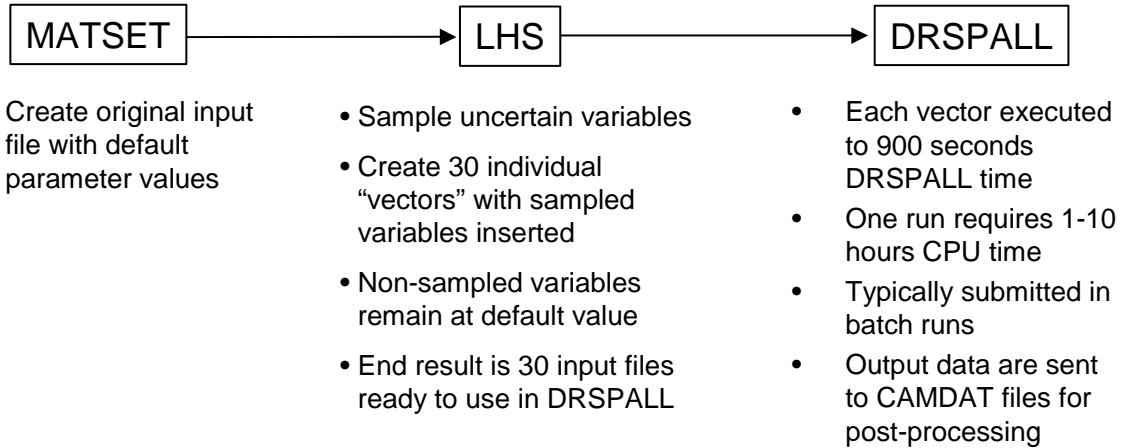


Figure 2-1. Code flow diagram for DRSPALL pre-processors.

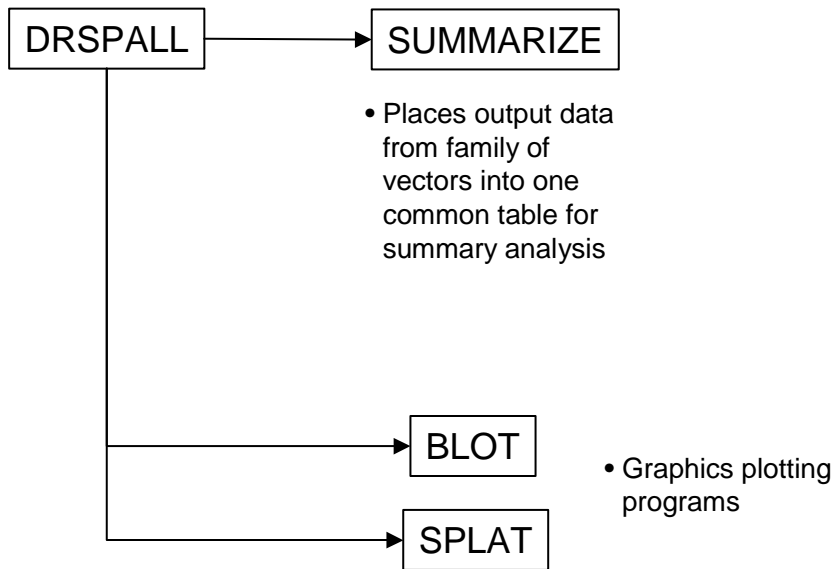


Figure 2-2. Code flow diagram for DRSPALL post-processors.

The second step requires running LHS to create 30 individual output vectors containing unique sets of input variables. The input to LHS includes the binary template created by MATSET and the input file LHS1\_DRSPALL.TRN, which gives the ranges and distribution types for sampled variables. Output from LHS appears in both ASCII and binary format. The ASCII file of most interest is the LHS2\_DRSPALL.TRN file that lists the results of the LHS sampling in tabular format. A listing of this file is given in Appendix LHS2\_DRSPALL.TRN. The binary output appears as 30 individual files ( 1 per vector) that serve as input to DRSPALL.

The next step requires submitting one DRSPALL run per vector. This is typically done in batch mode. This analysis ran 2 samples of 30 vectors each, requiring a total of 60 DRSPALL runs. All runs were executed to 900 seconds in DRSPALL time. This run time was determined by repeated trial and error in the model development process. Inspection of the output will reveal that drilling, tensile failure, fluidization, and spall releases to the surface all settle to steady values by 900 seconds. As such, there is no new information gained from running the code out longer.

Post-processing DRSPALL output takes two primary paths. The binary data from 30 runs can be summarized into one aggregate ASCII table for querying and analysis in a database or spreadsheet. Alternatively, the binary data may be read directly into a plotting program like BLOT (WIPP PA, 1996a), or preprocessed for input to SPLAT (WIPP PA, 1996b) for direct observation of history or spatial variables.

### **2.3 Output variable definitions**

A comprehensive list of variable definitions is given in Appendix VARIABLE GLOSSARY. Of interest in this sensitivity study are:

1. Radial variables
  - a. Cuttings radius (CUTRAD)
  - b. Cavity radius (CAVRAD)
  - c. Tensile radius (TENSRAD)
2. Pressure variables
  - a. Cavity pressure in repository (CAVPRS)
  - b. Flowing bottomhole pressure in wellbore (BOTPRS)
3. Equivalent uncompacted volumes
  - a. Total (TOTVOLEQ)
  - b. Cuttings (CUTVOLEQ)
  - c. Spallings (SPLVOLEQ)

#### **2.3.1 Radial variables**

The radius is a key variable to understand in the DRSPALL model because spatial variables in the 1-D cylindrical and spherical geometries are all expressed as a function of radius. The origin for the cylindrical geometry is a line down the center of the borehole denoting the axis of symmetry (Figure 2-3a). The origin for the spherical repository domain is a point where the axis of the drill bit first touches the top of the repository (Figure 2-3b). The three primary radial variables in DRSPALL output are the drill

cuttings radius, cavity radius, and the tensile-failed radius. The relationship among these three is demonstrated in Figure 2-3. The easiest place to start is with the cutting radius. This represents the position of the drill bit face in the repository. In most cases run here, drilling is the only mechanism that expands the cavity radius, so the drill radius and cavity radius will overlay. In the event of spallings, however, the cavity radius may actually grow larger than the drilled radius, as depicted in Figure 2-3. This implies that the spallings mechanism has removed material ahead of the drill bit. A third radial variable, tensile-failed radius, is also important to monitor because this variable identifies solid material that has failed due to the stress state, but has not mobilized into the flow stream. This may or may not be larger than the cavity radius, but it can never be smaller. Figure 2-3 and 2-4 show a situation in which material has failed out ahead of the bit, but has not fluidized and therefore forms a bed of disaggregated material subject to fluidization as the gas velocity reaches a sufficiently high value.

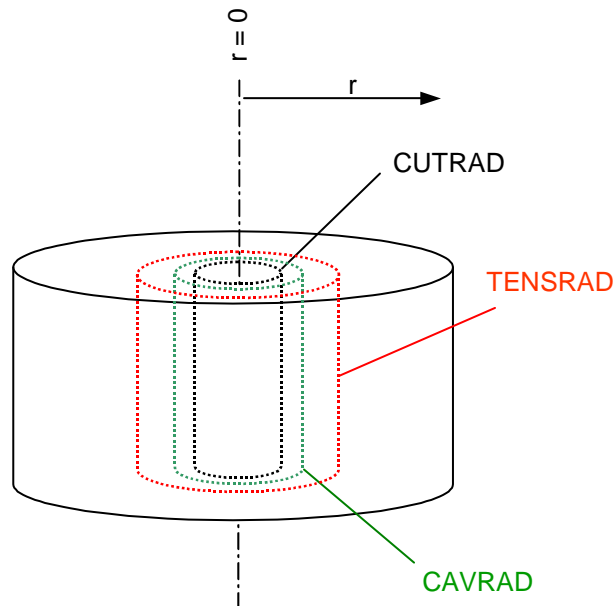


Figure 2-3. Radial variables in cylindrical geometry.

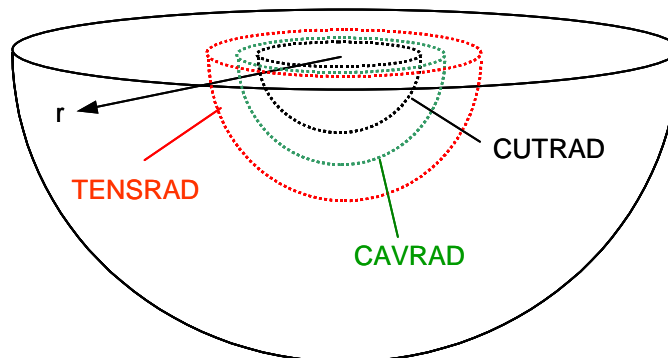


Figure 2-4. Radial variables in spherical geometry.

### 2.3.1.1 Mapping the cuttings radius in DRSPALL geometry

The cuttings radius in the one-dimensional DRSPALL geometry is mapped to the cuttings in a real three-dimensional system by conserving the surface area of the expanding cavity. For the cylindrical geometry, this involves starting with a narrow cylinder that extends through the repository height along the drilling axis, and expanding the radius as the real bit penetrates downward. For the spherical geometry, this requires defining a small hemisphere that has its origin at the point where the drillbit would first intersect the repository, and expanding this hemisphere radially as the bit proceeds. Drilling continues in both geometries for the amount of time required for a real bit to penetrate the entire depth of the repository. This implies that the rate of areal expansion of the drilled cavity is the same in all systems. More detail on the mapping among geometries is given in the Design Document for DRSPALL, document version 1.10 (WIPP PA, 2003).

### 2.3.2 Pressure variables

The two pressure variables of interest prior to bit penetration are the “pseudo-“ cavity pressure in the repository, and the flowing bottomhole pressure in the wellbore. The pseudo-cavity is a small volume created in the repository in order to avoid forcing the gas to flow to a single point (spherical geometry) or line (cylindrical geometry) at the origin of the domain. See the DRSPALL Design Document, v1,.10 (WIPP PA, 2003) for a more detailed explanation of the pseudo-cavity. Upon bit penetration, the cavity and well bottom define the same region in the model domain, and thus evaluate to the same pressure.

### 2.3.3 Equivalent volumes

DRSPALL calculates the mass of repository solids ejected to the land surface. For the purpose of comparing these release masses to releases from CCA and PAVT analyses, the DRSPALL expelled masses are converted to “equivalent uncompacted volume” units:

$$V_{eq} = \frac{m_s}{\rho_s(1 - \phi_o)} \quad (2.1)$$

where  $V_{eq}$  is the equivalent volume prior to compaction,  $m_s$  is the solids mass ejected at the surface,  $\rho_s$  is the solids density, and  $\phi_o$  is the porosity of a waste-filled room prior to closure. Values of  $\rho_s = 2650 \text{ kg/m}^3$  (Appendix DEFAULTS) and  $\phi_o = 0.85$  (DOE, 1996: Appendix PAR, Table PAR-38) are used in this analysis.

DRSPALL distinguishes between equivalent uncompacted volume of repository removed by all processes (TOTVOLEQ), and material released by spallings (SPLVOLEQ), by subtracting the equivalent volume of material removed by drilling action (CUTVOLEQ), or cuttings, from TOTVOLEQ. This is shown schematically for the hemispherical repository geometry in Figure 2-5.

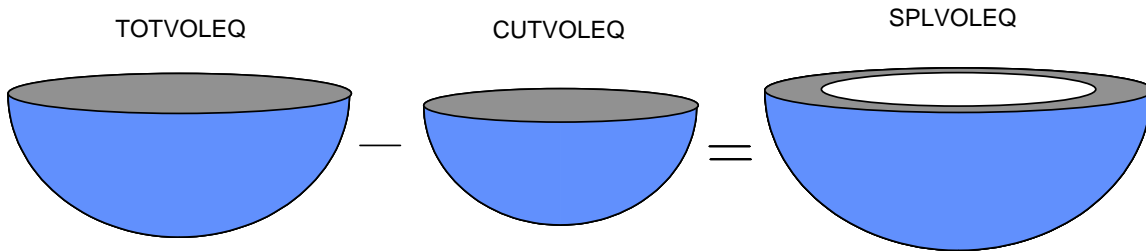


Figure 2-5. Schematic of the relationship among *TOTVOLEQ*, *CUTVOLEQ*, and *SPLVOLEQ*.

## 2.4 System specifications

This analysis was run on the Open VMS 7.3-1 operating system at Sandia National Laboratories, Carlsbad, NM. Runs were submitted to Compaq Alpha ES40, ES45, and 8400 machines, with a total of 20 processors available for computations. 60 vectors were executed in all, requiring about 277 hours of computational time spread over all 20 processors or roughly 48 hours of wall clock time.

## 3 RESULTS AND DISCUSSION – SPHERICAL GEOMETRY

### 3.1 First sample: Initial Repository Pressure = 8 – 15 MPa

The results of the first LHS sampling are summarized in Table 3-1. The 8-character variable names shown in the top row of Table 3-1 are defined in Appendix VARIABLE GLOSSARY. Note that the values for each variable fall within the bounds given in Table 2-1. The values in this table were extracted from the LHS output file LHS2\_DRSPALL.TRN, listed in its entirety in APPENDIX LHS2\_DRSPALL.TRN.

While there are many output variables of potential interest in the spallings model, the item of most concern from a TSPA and regulatory standpoint is the volume of spalled solids that is released to the surface. Shown in Table 3-2 is the summary of spallings releases for the 8-15 MPa runs. Note that only one vector (v007) gave a nonzero release, and the equivalent spalled volume is 0.24 m<sup>3</sup>.

Table 3.1. Results of 8-15 MPa LHS sampling. A glossary of variable names is given in Appendix VARIABLE GLOSSARY.

VEC	REPIPRES	REPIPOR	REPIPERM	POISRAT	TENSLSTR	INITMDEN	MUDVISCO	MUDSOLMX	MUDSOLVE	DRILRATE	MUDPRATE	DDZPERM	WALLROUG	SHAPEFAC	PARTDIAM
1	1.44E+07	5.38E-01	1.05E-12	4.11E-01	1.30E+05	1.29E+03	1.86E-02	6.28E-01	-1.66E+00	3.28E-03	2.20E-02	1.04E-15	4.28E-04	8.80E-01	7.88E-03
2	1.12E+07	5.97E-01	6.20E-14	4.00E-01	1.43E+05	1.26E+03	1.56E-02	6.00E-01	-1.77E+00	5.64E-03	2.13E-02	4.28E-14	1.19E-03	9.95E-01	6.90E-03
3	1.18E+07	5.64E-01	8.53E-13	3.57E-01	1.48E+05	1.22E+03	2.53E-02	5.97E-01	-1.67E+00	4.10E-03	1.77E-02	3.22E-14	1.61E-03	2.45E-01	8.13E-03
4	1.04E+07	6.09E-01	7.71E-13	3.82E-01	1.67E+05	1.32E+03	8.66E-03	6.19E-01	-1.71E+00	5.84E-03	1.67E-02	2.08E-14	6.69E-05	2.01E-01	5.91E-03
5	9.27E+06	5.00E-01	2.72E-13	4.17E-01	1.25E+05	1.31E+03	9.75E-03	6.10E-01	-1.26E+00	4.04E-03	1.76E-02	6.65E-15	2.60E-03	7.05E-01	4.51E-03
6	1.46E+07	6.35E-01	3.41E-13	3.83E-01	1.27E+05	1.37E+03	2.81E-02	5.93E-01	-1.39E+00	4.54E-03	2.25E-02	5.62E-14	8.78E-05	5.02E-01	7.27E-03
7	1.39E+07	3.93E-01	1.13E-13	4.19E-01	1.60E+05	1.27E+03	1.93E-02	6.34E-01	-1.54E+00	5.18E-03	2.10E-02	1.83E-15	1.53E-03	1.73E-01	8.77E-03
8	1.46E+07	4.53E-01	3.73E-13	3.85E-01	1.45E+05	1.20E+03	1.46E-02	6.40E-01	-1.44E+00	5.63E-03	1.88E-02	7.67E-14	2.11E-03	5.33E-01	4.71E-03
9	1.26E+07	5.68E-01	8.00E-14	4.03E-01	1.52E+05	1.25E+03	1.24E-02	6.29E-01	-1.36E+00	3.01E-03	1.74E-02	8.67E-14	5.51E-05	5.86E-01	6.61E-03
10	9.42E+06	3.75E-01	5.60E-13	4.23E-01	1.35E+05	1.35E+03	8.26E-03	6.06E-01	-1.79E+00	3.56E-03	2.17E-02	2.87E-14	1.02E-04	1.08E-01	2.33E-03
11	8.23E+06	4.34E-01	2.61E-13	4.29E-01	1.23E+05	1.20E+03	2.74E-02	6.37E-01	-1.69E+00	5.12E-03	2.28E-02	3.89E-14	1.28E-04	7.94E-01	3.52E-03
12	1.34E+07	4.65E-01	1.19E-12	3.64E-01	1.42E+05	1.23E+03	1.62E-02	6.31E-01	-1.61E+00	3.16E-03	1.66E-02	1.90E-15	2.20E-04	9.41E-01	5.62E-03
13	1.16E+07	5.52E-01	5.15E-14	3.59E-01	1.69E+05	1.34E+03	1.36E-02	6.21E-01	-1.50E+00	5.24E-03	2.36E-02	9.62E-15	5.95E-04	9.31E-01	2.98E-03
14	1.08E+07	4.60E-01	3.29E-14	4.08E-01	1.63E+05	1.26E+03	1.15E-02	5.99E-01	-1.23E+00	3.50E-03	2.32E-02	4.79E-14	1.17E-03	8.93E-01	6.15E-03
15	1.02E+07	3.69E-01	1.51E-13	3.51E-01	1.32E+05	1.28E+03	1.83E-02	6.27E-01	-1.43E+00	4.19E-03	2.20E-02	3.50E-15	1.98E-03	3.29E-01	3.22E-03
16	8.11E+06	4.93E-01	1.40E-13	3.54E-01	1.65E+05	1.31E+03	2.97E-02	6.22E-01	-1.54E+00	4.35E-03	2.07E-02	5.00E-15	8.58E-05	6.76E-01	4.90E-03
17	1.40E+07	4.15E-01	2.66E-14	3.98E-01	1.55E+05	1.36E+03	1.32E-02	5.97E-01	-1.76E+00	3.07E-03	2.11E-02	2.27E-15	7.88E-04	6.56E-01	2.62E-03
18	9.61E+06	3.59E-01	4.73E-13	3.72E-01	1.36E+05	1.37E+03	2.50E-02	6.32E-01	-1.26E+00	4.85E-03	2.03E-02	6.87E-14	4.54E-04	5.76E-01	8.20E-03
19	1.05E+07	5.12E-01	2.24E-13	4.26E-01	1.54E+05	1.34E+03	2.61E-02	6.04E-01	-1.31E+00	5.34E-03	1.63E-02	1.24E-15	2.99E-04	7.34E-01	5.26E-03
20	1.23E+07	6.01E-01	1.78E-13	3.70E-01	1.20E+05	1.32E+03	1.07E-02	6.12E-01	-1.21E+00	4.96E-03	1.94E-02	3.16E-15	1.52E-04	2.93E-01	1.48E-03
21	1.31E+07	5.21E-01	3.08E-14	4.22E-01	1.61E+05	1.15E+03	2.37E-02	6.17E-01	-1.33E+00	4.58E-03	2.00E-02	1.08E-14	3.65E-04	4.33E-01	1.06E-03
22	1.26E+07	5.34E-01	1.76E-14	3.91E-01	1.33E+05	1.18E+03	2.87E-02	6.17E-01	-1.51E+00	3.86E-03	1.90E-02	2.82E-15	1.44E-04	1.50E-01	9.71E-03
23	9.96E+06	6.53E-01	3.77E-14	3.79E-01	1.30E+05	1.30E+03	2.23E-02	6.24E-01	-1.74E+00	3.73E-03	1.91E-02	2.31E-14	3.09E-03	2.74E-01	4.15E-03
24	8.85E+06	6.27E-01	6.76E-13	4.12E-01	1.41E+05	1.24E+03	1.73E-02	6.13E-01	-1.28E+00	4.29E-03	2.39E-02	1.43E-15	6.83E-04	6.34E-01	9.20E-03
25	8.49E+06	6.47E-01	7.24E-14	3.75E-01	1.47E+05	1.17E+03	5.23E-03	6.36E-01	-1.46E+00	3.81E-03	1.97E-02	7.85E-15	5.39E-04	4.24E-01	7.36E-03
26	8.95E+06	4.05E-01	1.30E-12	3.88E-01	1.59E+05	1.15E+03	2.33E-02	5.91E-01	-1.57E+00	3.39E-03	1.81E-02	1.60E-14	9.20E-04	4.84E-01	3.88E-03
27	1.12E+07	4.81E-01	2.00E-14	3.66E-01	1.22E+05	1.19E+03	2.13E-02	6.02E-01	-1.59E+00	5.47E-03	1.70E-02	1.39E-14	1.83E-04	7.68E-01	1.85E-03
28	1.29E+07	3.83E-01	1.03E-13	3.62E-01	1.28E+05	1.19E+03	6.80E-03	6.12E-01	-1.63E+00	4.68E-03	2.31E-02	4.13E-15	6.06E-05	8.45E-01	8.93E-03
29	1.35E+07	5.78E-01	1.50E-12	3.93E-01	1.50E+05	1.16E+03	2.05E-02	6.07E-01	-1.38E+00	4.81E-03	2.42E-02	5.41E-15	2.29E-04	3.59E-01	2.13E-03
30	1.20E+07	4.28E-01	4.33E-14	4.03E-01	1.39E+05	1.24E+03	6.17E-03	5.94E-01	-1.40E+00	5.79E-03	1.84E-02	1.33E-14	2.94E-04	3.82E-01	9.66E-03

Table 3-2. Summary of equivalent uncompacted spall volumes ( $m^3$ ) calculated for the 8-15 MPa sensitivity runs.

Vector	SPLVOLEQ	Vector	SPLVOLEQ
20	0	14	0
7	0.2386	16	0
15	0	17	0
1	0	18	0
2	0	19	0
3	0	21	0
4	0	22	0
5	0	23	0
6	0	24	0
8	0	25	0
9	0	26	0
10	0	27	0
11	0	28	0
12	0	29	0
13	0	30	0

In addition to looking at the summary output, it is instructive to review the progress of selected individual vectors in order to better understand the mechanisms controlling the release volumes. Vectors 020 and 007 are chosen here for a closer look.

### 3.1.1 Vector 020

Vector 020 has an initial repository pressure of  $P_1 = 12.3$  MPa, and a resulting equivalent uncompacted spall volume of  $SPLVOLEQ = 0$   $m^3$ . The following series of three figures (Figures 3-1 to 3-3) monitors the progress of several history variables. Included are plots of fluid pressure, radii of repository features, and uncompacted volumes.

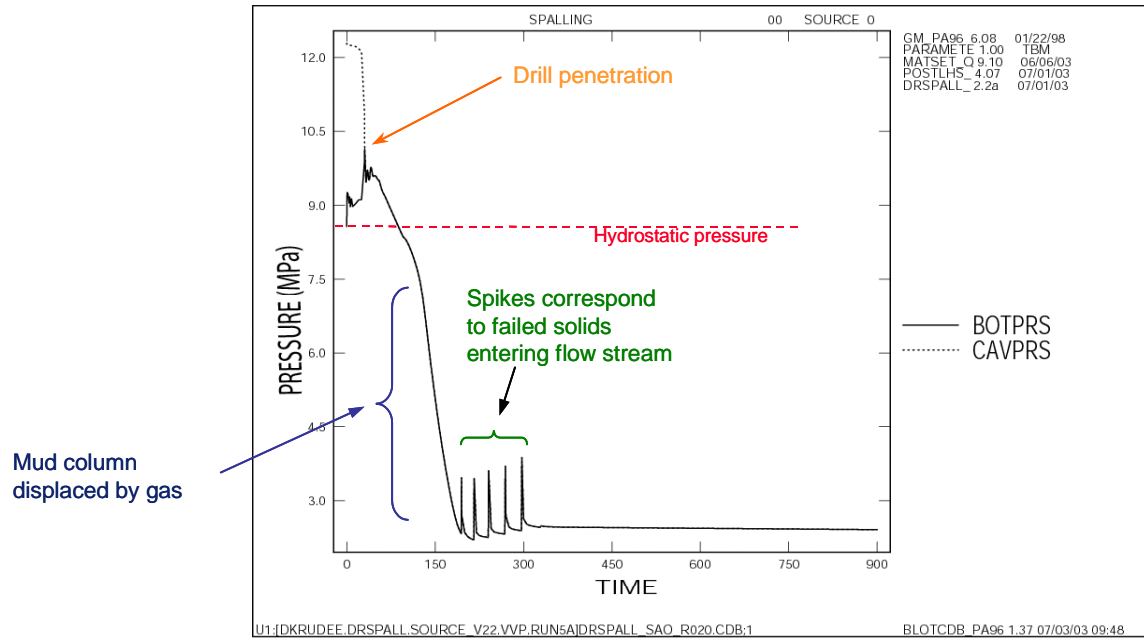


Figure 3-1. Pressure history plot for v020.

Figure 3-1 displays the history variables well bottomhole pressure (BOTPRS) and cavity pressure (CAVPRS) for vector 020. Labeled for reference on this plot is the hydrostatic pressure at the well bottom. Notice that at time = 0, the well starts near hydrostatic pressure, while the cavity pressure representing the face of the repository soon to be penetrated by the drill bit starts at 12.3 MPa (sampled initial repository pressure, REPIPRES). As time progresses and the drill bit approaches the repository, the pressures converge due to gas bleed through the DDZ and become equivalent when the drill actually penetrates the repository. The bottomhole pressure continues to drop as the mud column is displaced by gas and blown out of the borehole. In the field, this circumstance would be recognized by the driller as an increasing mud return rate provoking the closing of the blowout preventer. For the purpose of the WIPP PA, driller intervention is precluded and no steps are therefore taken by the hypothetical driller. Once the mud is displaced, the bottomhole pressure stabilizes to less than 3 MPa as gas blowdown continues. Several spikes in the pressure plot appear between 150 and 300 seconds. These correspond to solids failure and entrainment into the flow stream. Combined factors such as increases in mixture density, mixture viscosity, and numerical noise upon addition of discrete quantities of solids to the largely gas flow stream cause the spikes.

Figure 3-2 displays three radii that describe the progress of drilling (CUTRAD), material failure (TENS RAD), and cavity growth (CAVRAD) in the hemispherical repository domain. All radii start at zero and remain there until the bit intersects the repository at about 40 seconds. The drill bit proceeds though the repository domain until drilling stops at about 320 seconds. The endpoint for drilling is set by the simple formula:

$$\text{drilling time} = \text{repository height} / \text{drill penetration rate} \quad (3.1)$$

Repository height varies with porosity, and porosity is a sampled variable. As such, repository height is an indirectly sampled variable. In figure 3-2, the final drilled radius is about 0.49 m. Between 175 and 300 seconds, some stepping of the CAVRAD and TENSRAD variables is observed. This indicates that several tensile failure events expand the cavity momentarily ahead of the drill bit, but drilling eventually catches up so that all three variables overlay after 320 seconds. These steps will also correspond with the spikes observed in the pressure history plot (Figure 3-1).

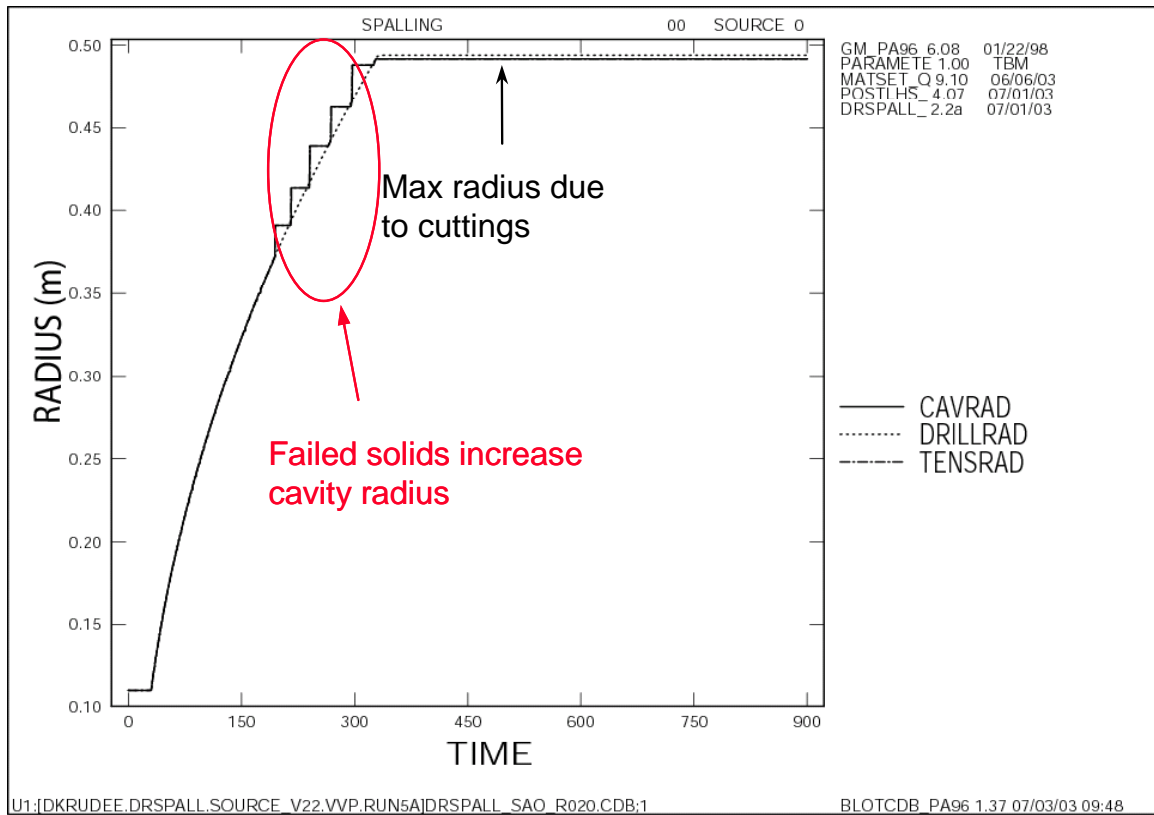


Figure 3-2. Radius variables history plot for v020.

Equivalent uncompacted volumes for v020 are shown as a function of time in Figure 3-3. Three variables, CUTVOLEQ, SPLVOLEQ, and TOTVOLEQ are displayed. All start at zero, and only increase after drilling begins in the repository at ~40 seconds. Notice that CUTVOLEQ and TOTVOLEQ overlay while SPLVOLEQ = 0 until about 175 seconds when the first spalling failure occurs. SPLVOLEQ spikes five times between 175 and 320 seconds, but in every case, drilling eventually excavates the volume spalled and the total spalled volume is reduced to zero. While the material removed by spalling is actually transported up the borehole as soon as it is fluidized, the mass accounting in the code assumes that such material would have eventually been removed by drilling, and therefore is not counted as spalled material in the final report at 900 seconds.

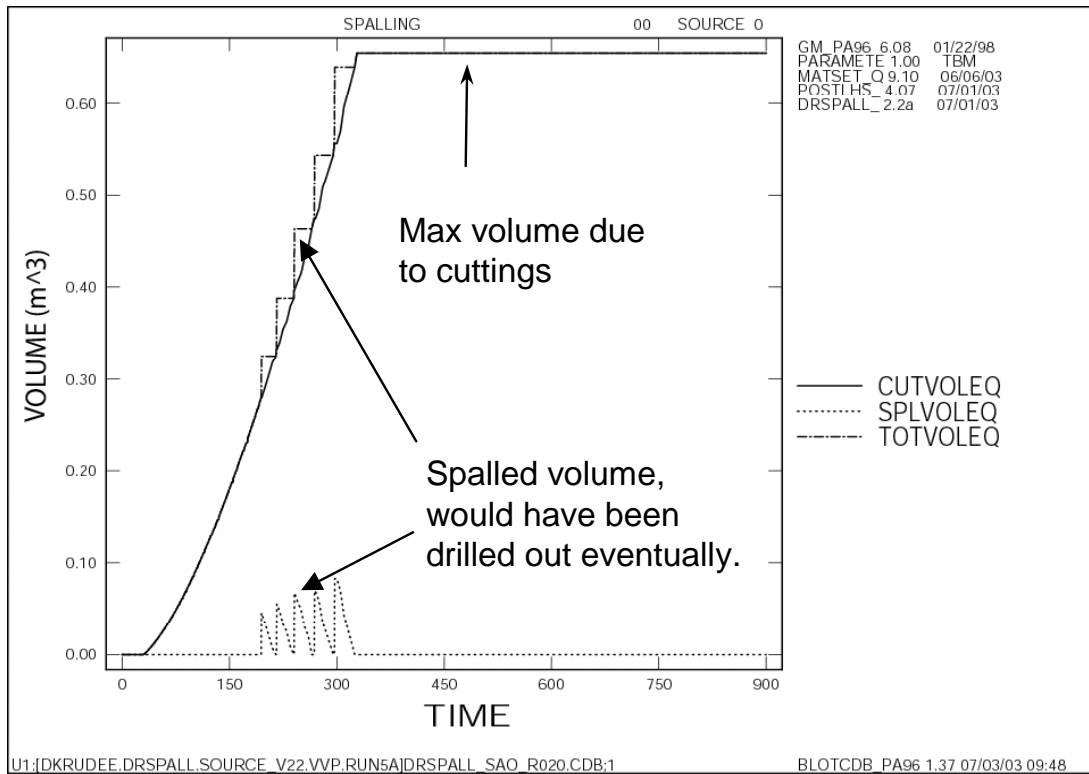


Figure 3-3. Equivalent volumes history plot for v020.

### 3.1.2 Vector 007

While vector 020 exhibited no ultimate spallings volumes at 900 seconds, vector 007 did have a final volume of  $SPLVOLEQ = 0.24 \text{ m}^3$ . Here we inspect the history variables in v007 closely to see what leads to a spalling event.

Figure 3-4 shows the pressures as a function of time. Repository pressure and bottomhole pressure converge at the time of drill penetration. Similarly to v020, the mud column blows out and bottomhole pressure decreases to below 3.0 MPa. Also, some temporary spall failure is indicated by the spikes between 175 and 300 seconds.

Figure 3-5 shows that the three radii of interest for vector 007 overlay until about 200 seconds when the tensile and cavity radii expand to  $\sim 0.46 \text{ m}$ . The drilling stops at  $\sim 0.40 \text{ m}$ , resulting in spalled material at 900 seconds. The match between the cavity radius and tensile radius implies that fluidization occurs immediately after tensile failure. Inspection of the superficial gas velocity ( $WBSUPVEL$ ) relative to the minimum fluidization velocity ( $FLUIDVEL$ ) in Figure 3-6 confirms that fluidization should occur at virtually all times after 150 seconds.

Final equivalent uncompacted volumes for v007 are shown in Figure 3-7. The final cavity volume is  $0.79 \text{ m}^3$ , and after subtracting cuttings, the remaining spalled volume is  $0.24 \text{ m}^3$ .

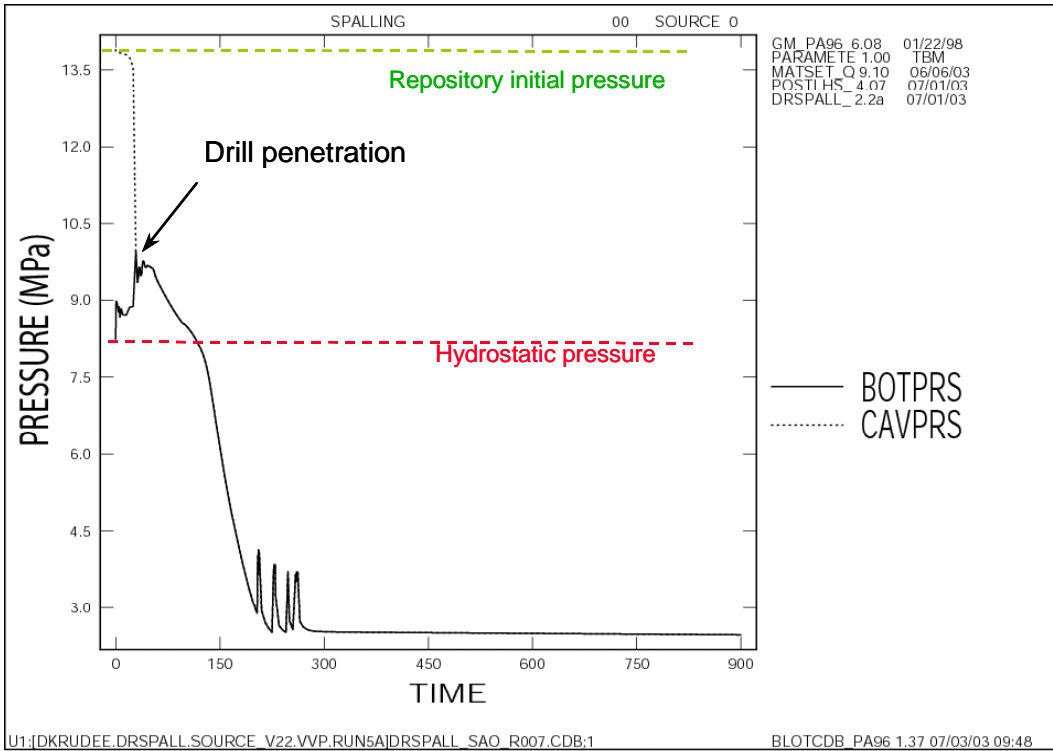


Figure 3-4. Pressure history plot for v007.

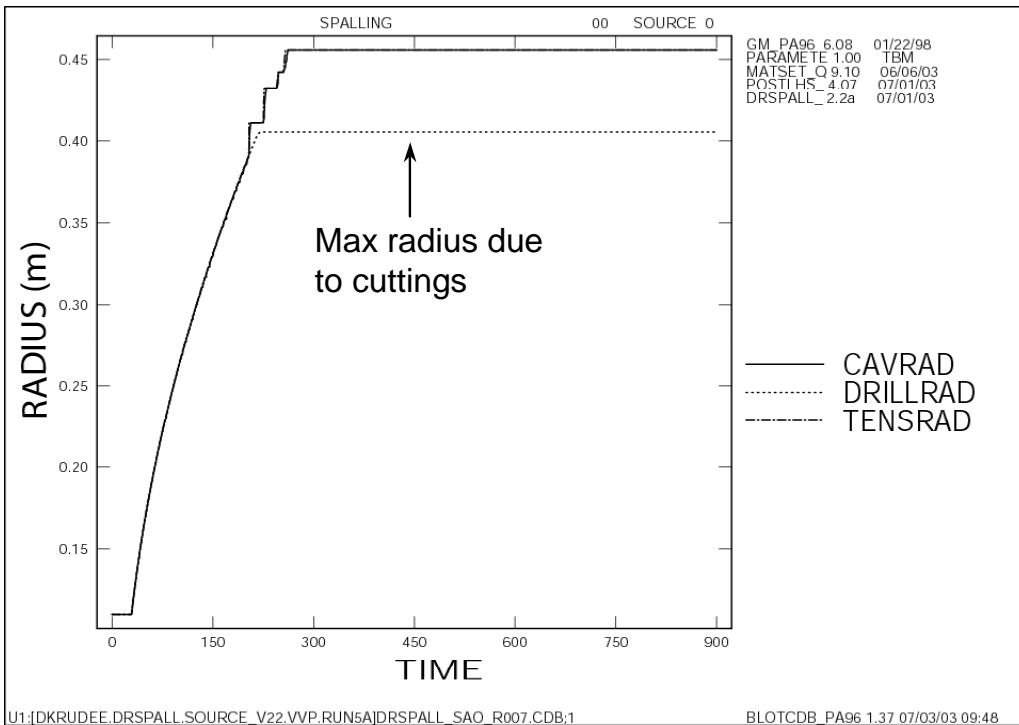


Figure 3-5. Radius variables history plot for v007.

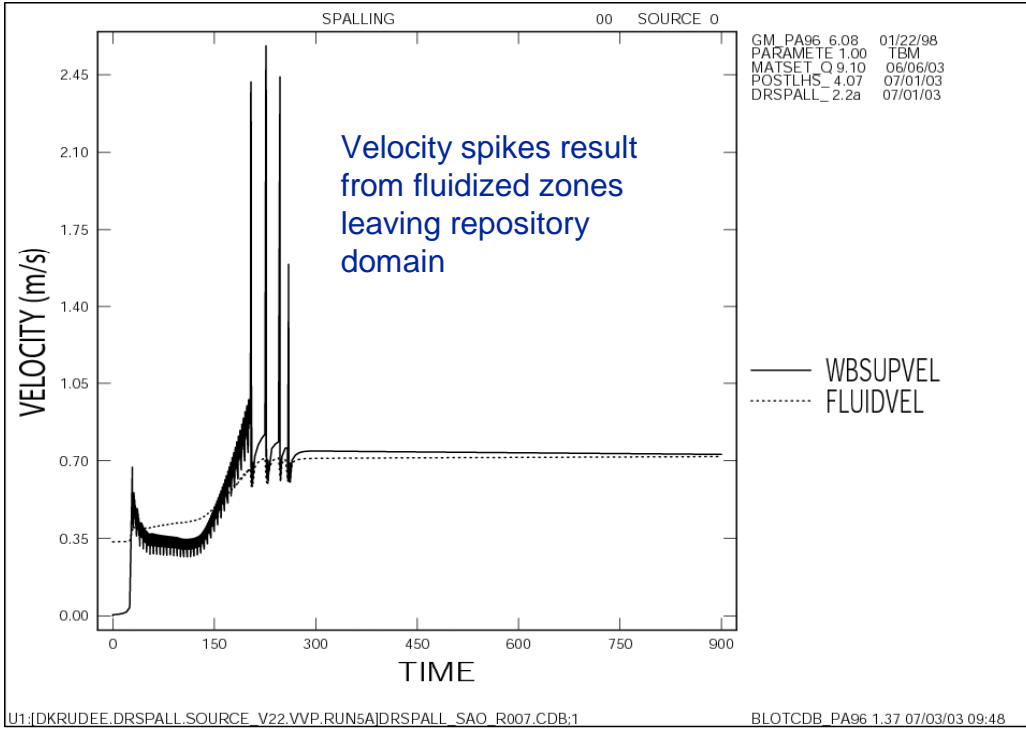


Figure 3-6. Velocity history plot for v007.

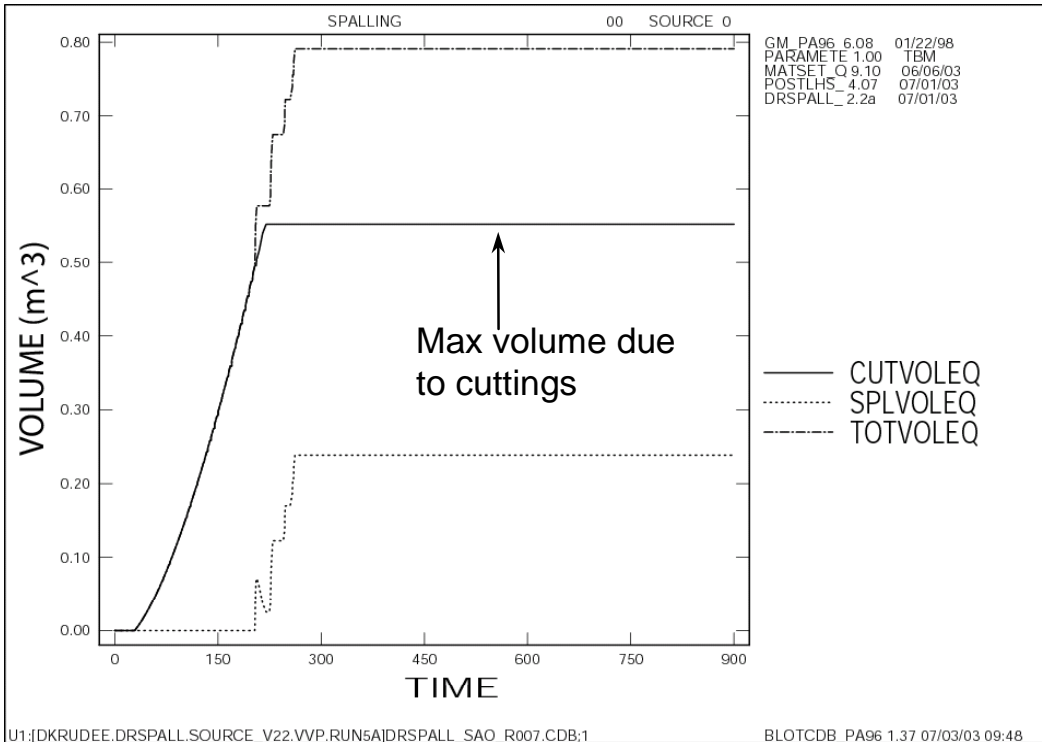


Figure 3-7. Equivalent uncompacted volume plot for v007.

### 3.2 Second sample: Initial Repository Pressure = 12 – 15 MPa

The range for repository initial pressure is the only variable that changes in this sampling, now raised to 12-15 MPa. As such, all of the other values will be the same vector-by-vector (see Table 3-1). The new pressure sampling is shown in Table 3-3.

*Table 3-3. Sampled pressures for high-pressure sensitivity matrix.*

<b>vector</b>	<b>Repository Pressure (Pa)</b>	<b>vector</b>	<b>Repository pressure (Pa)</b>
<b>1</b>	1.47E+07	<b>16</b>	1.20E+07
<b>2</b>	1.33E+07	<b>17</b>	1.45E+07
<b>3</b>	1.36E+07	<b>18</b>	1.27E+07
<b>4</b>	1.30E+07	<b>19</b>	1.31E+07
<b>5</b>	1.25E+07	<b>20</b>	1.38E+07
<b>6</b>	1.47E+07	<b>21</b>	1.41E+07
<b>7</b>	1.45E+07	<b>22</b>	1.39E+07
<b>8</b>	1.48E+07	<b>23</b>	1.28E+07
<b>9</b>	1.39E+07	<b>24</b>	1.24E+07
<b>10</b>	1.26E+07	<b>25</b>	1.22E+07
<b>11</b>	1.21E+07	<b>26</b>	1.24E+07
<b>12</b>	1.43E+07	<b>27</b>	1.33E+07
<b>13</b>	1.35E+07	<b>28</b>	1.40E+07
<b>14</b>	1.32E+07	<b>29</b>	1.43E+07
<b>15</b>	1.29E+07	<b>30</b>	1.37E+07

When executed in DRSPALL, these 30 vectors resulted in just three nonzero releases. The summary results are presented in Table 3-4. Note that v007 was again a release vector, with a doubling of release volume observed with an increase in pressure from 13.9 to 14.5 MPa. Vectors 020 and 015 now exhibit nonzero releases, with values of 1.20 and 0.05 m<sup>3</sup> equivalent uncompacted spall volumes, respectively.

Table 3-4. Summary of equivalent uncompacted spall volumes ( $m^3$ ) calculated for the 8-15 MPa and 12-15MPa sensitivity runs.

Vector	SPLVOLEQ		Vector	SPLVOLEQ	
	8-15 MPa	12-15 MPa		8-15 MPa	12-15 MPa
20	0	1.2026	14	0	0
7	0.2386	0.49153	16	0	0
15	0	0.049454	17	0	0
1	0	0	18	0	0
2	0	0	19	0	0
3	0	0	21	0	0
4	0	0	22	0	0
5	0	0	23	0	0
6	0	0	24	0	0
8	0	0	25	0	0
9	0	0	26	0	0
10	0	0	27	0	0
11	0	0	28	0	0
12	0	0	29	0	0
13	0	0	30	0	0

### 3.2.1 Vector 020, high pressure

Initial repository pressure was increased relative to the first run from 12.3 MPa to 13.8 MPa. This resulted in an increase in SPLVOLEQ from 0 to 1.2  $m^3$ . Starting with the radius variables (Figure 3-8), it is evident that the tensile and cavity radii separate from the drilled radius after 150 seconds and climb to a stable value of  $\sim 0.70$  m. Recall that the initiation of failure in the low-pressure v020 (Figure 3-2) also occurred around 150 seconds, but the stress state induced by the lower pressure gradient was not sufficient to propagate the failure more than 2 or 3 cm ahead of the drill bit. In the high-pressure case, the failure and subsequent fluidization (Figure 3-9) caused the cavity to grow rapidly to a radius of 0.70 m, where it then stabilized. The fact that the cavity growth ceased but superficial velocity exceeds fluidization velocity implies that the cavity is stabilized by the stress state, with no more failure occurring. Any failed and bedded material has been entrained and transported to the surface.

Volume history for v020, high pressure, is shown in Figure 3-10. At 150 seconds, the TOTVOLEQ grows along with the cavity radius to a stable volume of  $\sim 1.8$   $m^3$ . SPLVOLEQ reaches a peak of  $\sim 1.4$   $m^3$  at 250 seconds, but decreases to 1.2  $m^3$  as the drill excavates some of the volume that spalled.

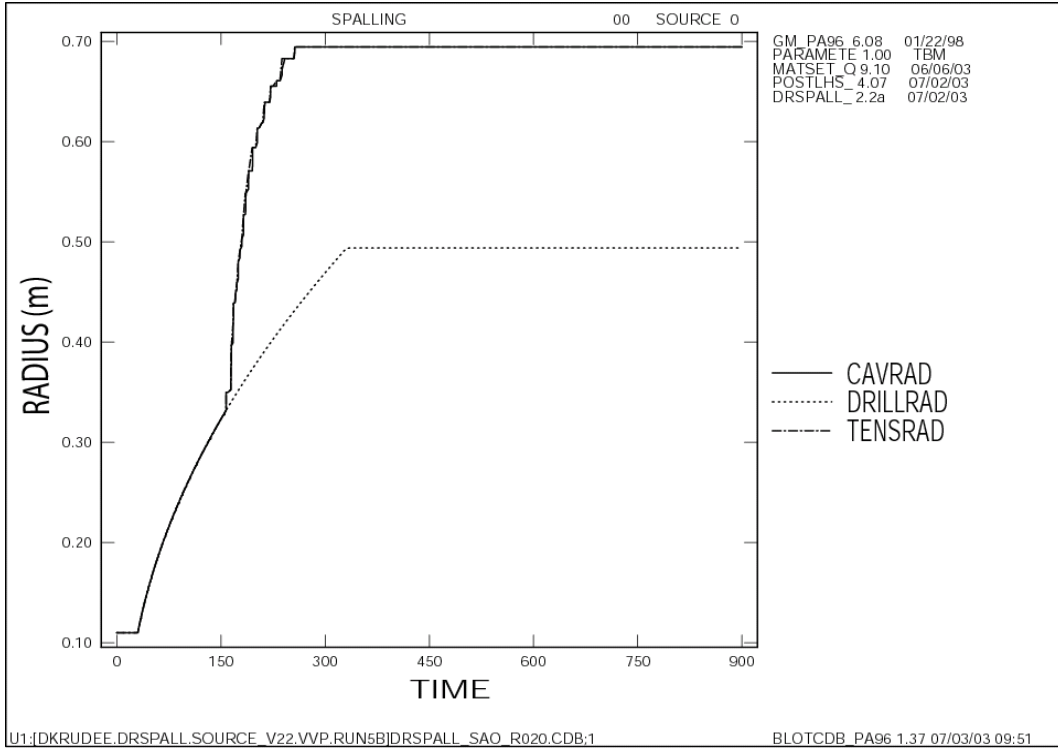


Figure 3-8. Radius variables history plot for v020, high pressure case.

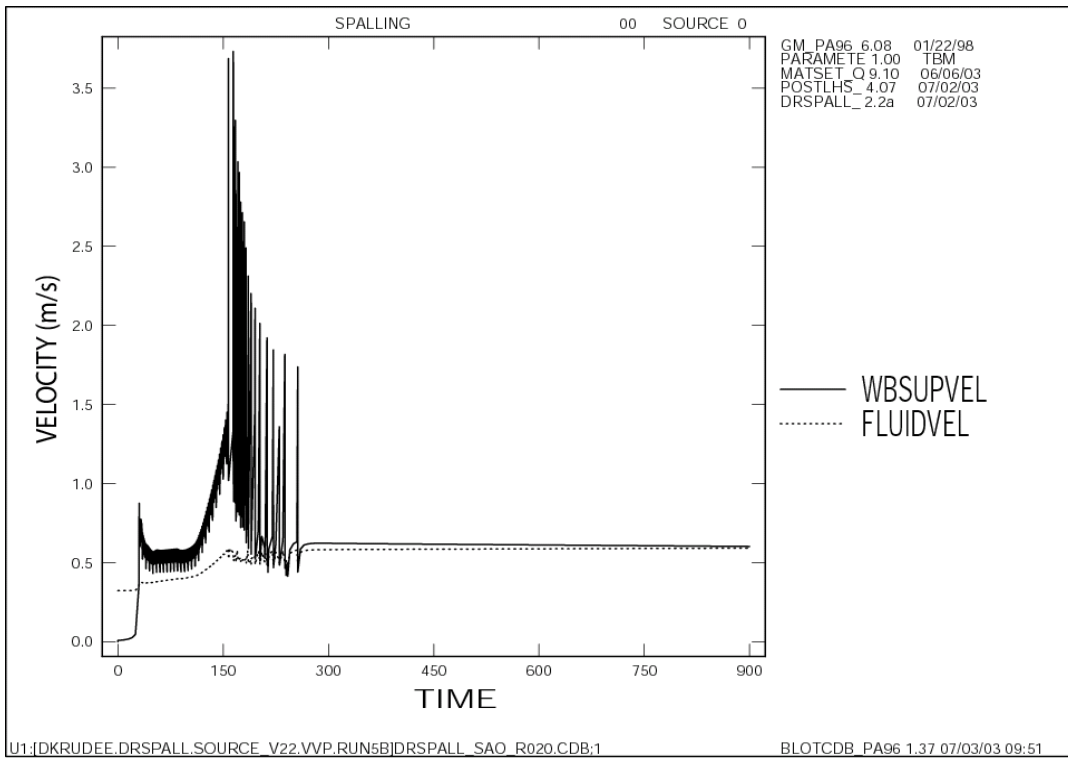


Figure 3-9. Velocity history plot for v020, high pressure case.

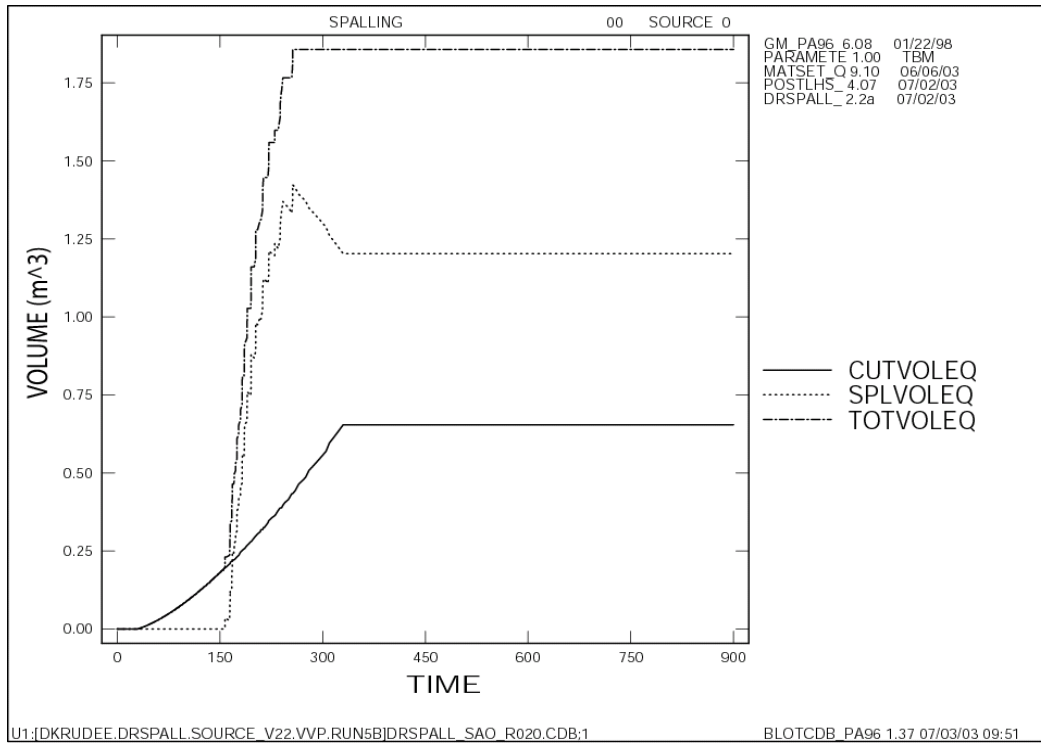


Figure 3-10. Equivalent uncompacted volume history plot for v020, high pressure case.

### 3.2.2 Vector 007, high pressure

A doubling of spall volume was observed in v007 due to an increase in repository pressure from 13.9 to 14.5 MPa. Inspection of the radius variables plot (Figure 3-11) shows that the failed radius settles to a slightly larger value (0.51 m) than the cavity radius (0.50 m), while the drilled radius stopped at 0.40 m. There is apparently failed, bedded material in this vector that does not entrain into the wellbore flow stream. Confirmation of this can be found in the velocity history plot (Figure 3-12), where the superficial velocity lies below the minimum fluidization velocity after 300 seconds. This cavity is therefore stabilized by the fluidized bed mechanism. The equivalent uncompacted cavity volume stabilized to  $TOVOLEQ = 1.05 \text{ m}^3$  after 300 seconds, while the equivalent uncompacted spall volume reached a stable value of  $SPLVOLEQ = 0.49 \text{ m}^3$ .

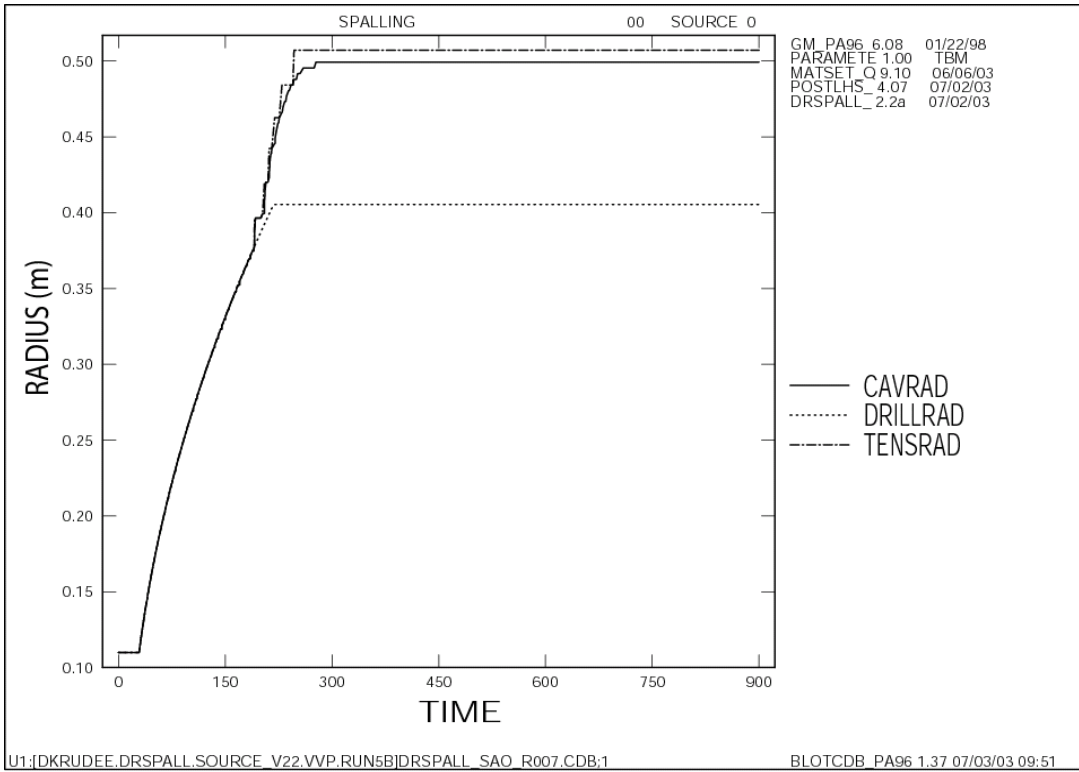


Figure 3-11. Radius variables history plot for v007, high pressure case.

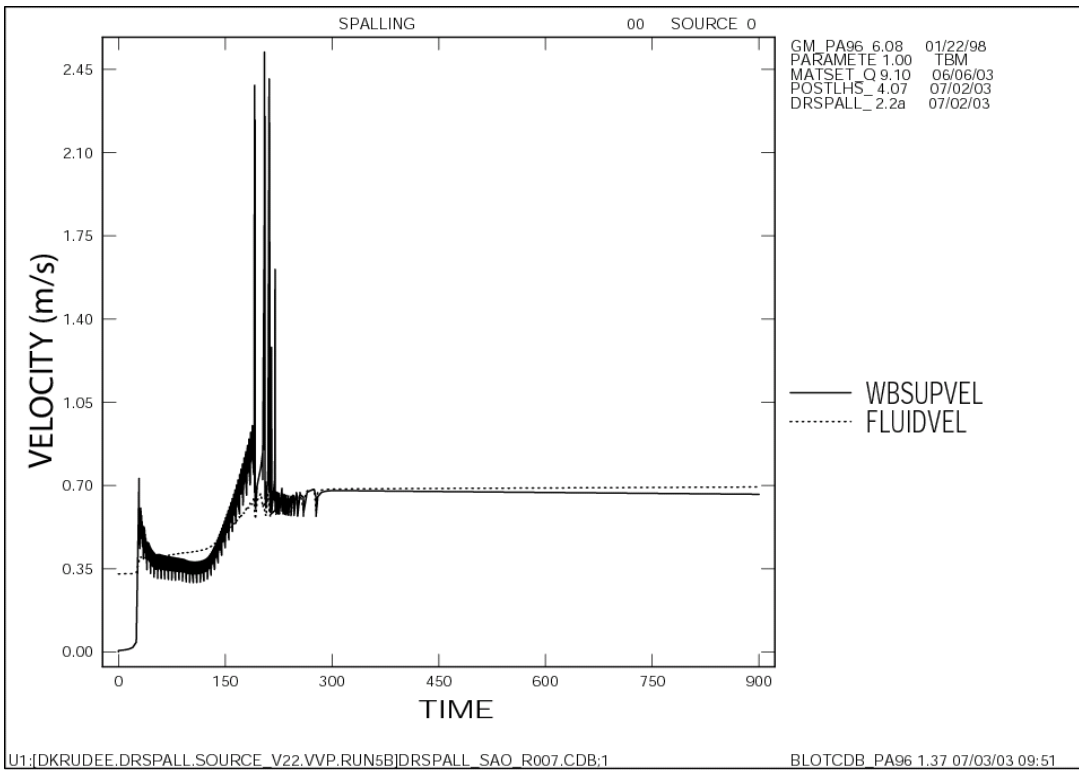


Figure 3-12. Velocity history plot for v007, high pressure case.

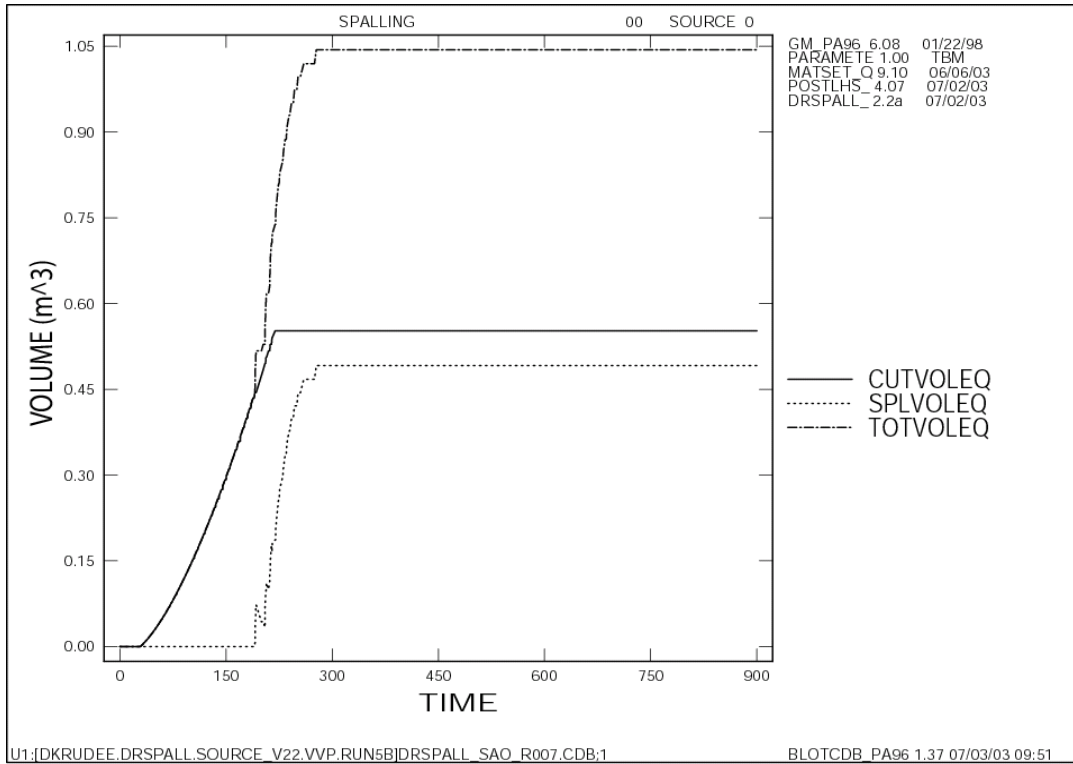


Figure 3-13. Equivalent uncompact volume history plot for v007, high pressure case.

### 3.3 Scatterplots

In addition to reviewing lists of final output variables, model sensitivity may also be explored by using scatterplots. A selected dependent variable such as equivalent uncompact spall volume (SPLVOLEQ) at a late time in the run, typically 900 seconds, is plotted as a function of an independent variable such as initial repository pressure (REPIPRES). In this format, it is possible to explore possible correlations between the input and output variable by visual inspection the results of all 60 vectors on one set of axes. For the data shown here, the following dependent variables were explored:

- equivalent uncompact spall volume
- tensile radius – cutting radius

...as a function of the following independent variables:

- repository initial pressure
- repository permeability
- waste tensile strength
- particle diameter × shape factor

### 3.3.1 Variables controlling equivalent uncompacted spall volume

#### 3.3.1.1 Repository initial pressure

Figure 3-14 shows SPLVOLEQ at 900 seconds plotted as a function of REPIPRES. Each symbol in this figures corresponds to one vector, so there are 60 symbols on this plot. While only 4 vectors of the 60 give nonzero spall releases, it is apparent that no vectors with REPIPRES < 12 MPa exhibited spillings. Repository pressure is a critical variable in the spillings model for several reasons. First, the stress state in the porous solid is a direct function of the pressure gradient formed between the far field and the wellbore. A larger pressure gradient leads to higher stresses and more potential failure. Second, mobilization of tensile-failed solids requires a sufficient gas velocity for the loose particles to mobilize into the flow stream by fluidized bed theory. A minimum fluidization velocity defined by the Ergun (1952) model must be exceeded in order to mobilize waste. The gas velocity at the cavity face that causes fluidization is directly proportional to the pressure gradient at the cavity wall. Therefore, the repository pressure relative to the wellbore pressure is a critical variable impacting the equivalent uncompacted spall volume releases.

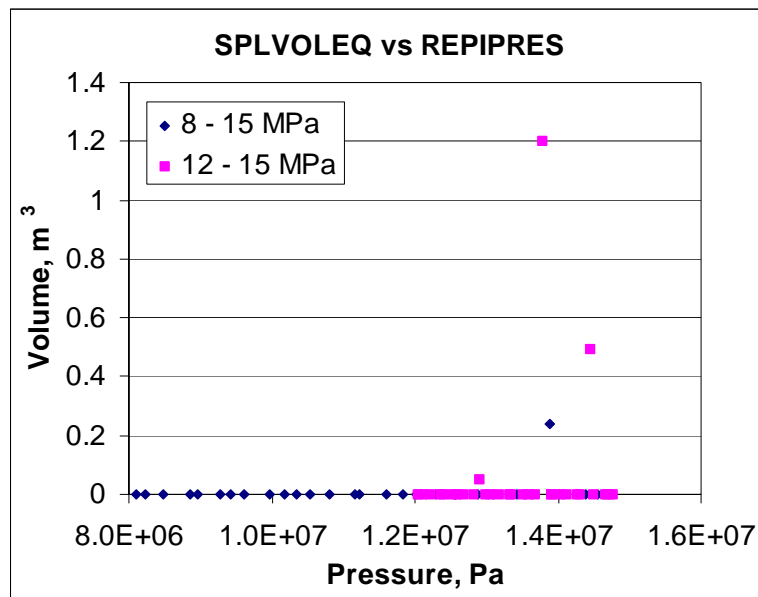


Figure 3-14. Scatterplot of SPLVOLEQ vs. REPIPRES for all 60 vectors.

#### 3.3.1.2 Waste tensile strength

Also potentially important in determining SPLVOLEQ is the tensile strength of waste. Figure 3-15 shows a scatterplot with TENSLSTR as the independent variable. With only four release vectors out of 60, the data above the zero axis are sparse, and it is difficult to find a correlation. The highest release did coincide with the lowest tensile strength vector (v020) from the high-pressure runs (REPIPRES = 13.8 MPa), but no release was observed for the same vector at a slightly lower pressure (REPIPRES = 12.3 MPa).

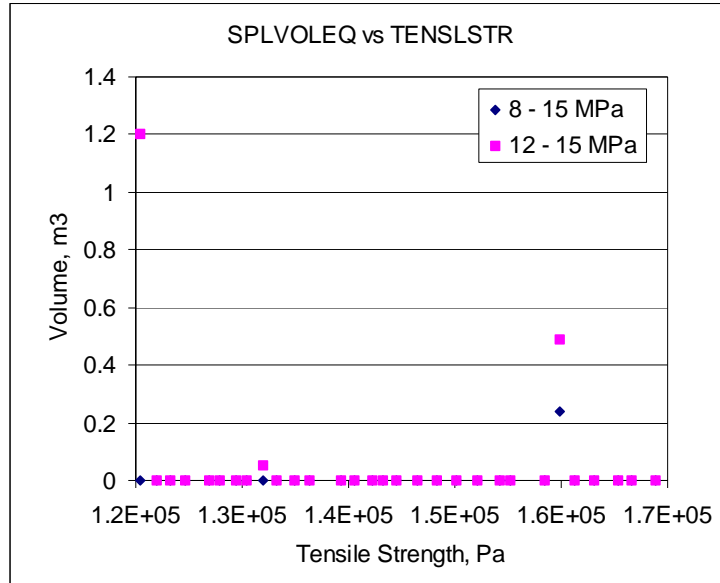


Figure 3-15. Scatterplot of *SPLVOLEQ* vs. *TENSLSTR* for all 60 vectors.

### 3.3.1.3 Particle diameter and shape factor

Particle diameter and shape factor can become important to spall release volumes through their impact on the minimum fluidization velocity calculated by Ergun's equation (Ergun, 1952, Hansen et al., 2003). These two factors appear as a product in Ergun's model, and have the general effect of lowering the minimum fluidization velocity as their product is lowered. In physical terms, small or non-spherical particles in a packed bed are more likely to fluidize than large, spherical particles. The scatterplot shown in Figure 3-16 shows the relationship between the product *PARTDIAM\*SHAPEFAC* and the equivalent uncompact spall volume. It is difficult from this figure to clearly identify a relationship between the independent and dependent variables. Note that the independent variable axis is plotted on a logarithmic scale, so most of the activity appears to occur below a product of  $2.0E-3$  m. Recall that particle diameter is varied from 1 mm to 1 cm, while shape factor is varied from 0.1 to 1.0. There is no conclusive relationship indicated in this figure.

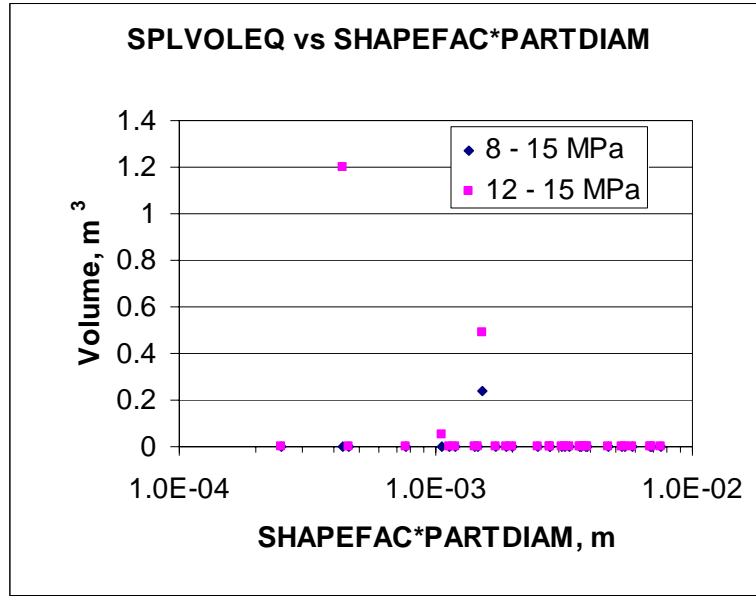


Figure 3-16. Scatterplot of SPLVOLEQ vs. SHAPEFAC\*PARTDIAM for all 60 vectors.

### 3.3.2 Variables controlling tensile radius

It is illustrative for this analysis to define a new dependent variable by computing the difference between the tensile-failed radius and the cavity radius. This new variable is depicted schematically in Figure 3-17. While not of particular interest to TSPA results, the difference between these two variables indicates the extent to which the repository material failed ahead of the ultimate drilled radius. This gives an indication of the potential for spallings, independent of how much material was actually moved up the borehole. Tensile failure is a necessary precursor to spall release. In this sensitivity sample where the spall releases are mostly zero, this new intermediate variable helps to visualize the coupled mechanisms that control spall releases, and provides more resolution to the output.

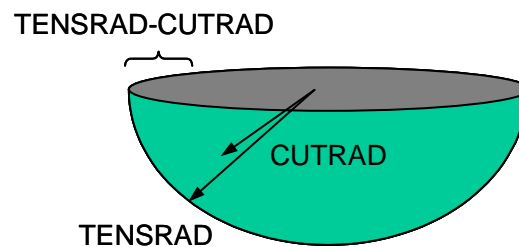


Figure 3-17. Schematic of definition of TENS RAD-CUT RAD output variable.

#### 3.3.2.1 Repository initial pressure

The sensitivity of TENS RAD-CUT RAD to repository initial pressure is illustrated in Figure 3-18. Notice that a distinct break occurs at about 11 MPa. Below this pressure, no failure was observed in any vector. Above this pressure, about half of the vectors

exhibited failure. This indicates a strong relationship between pressure and failure, consistent with the design of the conceptual model.

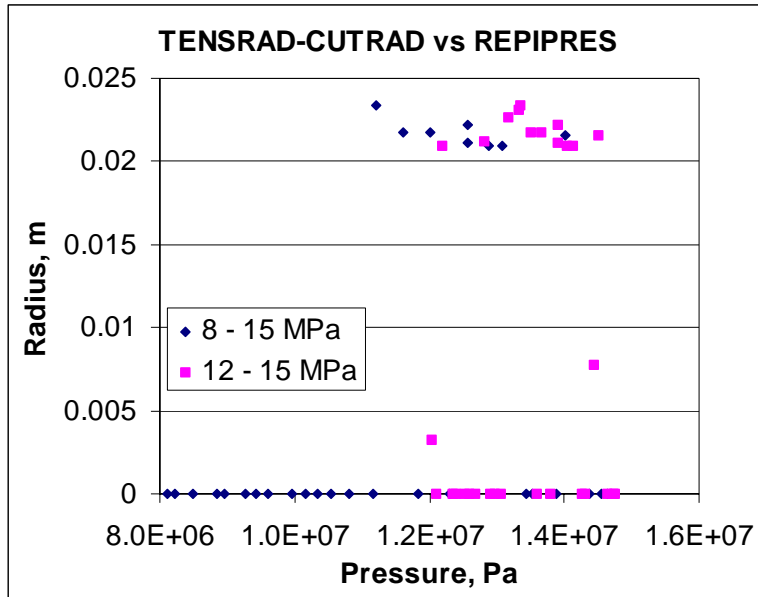


Figure 3-18. Scatterplot of TENSRAD-CUTRAD vs. REPIPRES for all 60 vectors.

3.3.2.2 Tensile strength

The sensitivity of TENSRAD-CUTRAD to waste tensile strength is illustrated in Figure 3-19. No particular correlation is observed, with failure apparently just as likely over the range of tensile strength (0.12-0.17 MPa) examined.

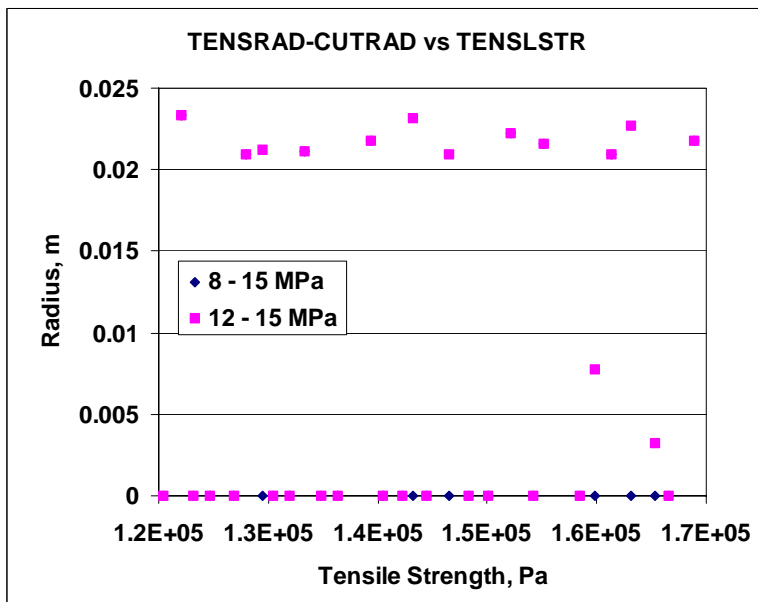


Figure 3-19. Scatterplot of TENSRAD-CUTRAD vs. TENSSTR for all 60 vectors.

### 3.3.2.3 Repository permeability

Plotting the TENS RAD-CUTRAD against repository permeability illustrates an important relationship in the spillings model. No failure is observed for waste material with permeability above  $k = 2\text{E-}13 \text{ m}^2$ . Alternatively, many failures are observed at permeability below  $k = 2\text{E-}13 \text{ m}^2$ . This is consistent with the design of the conceptual model that would suggest more failure due to higher pressure gradients in less permeable media.

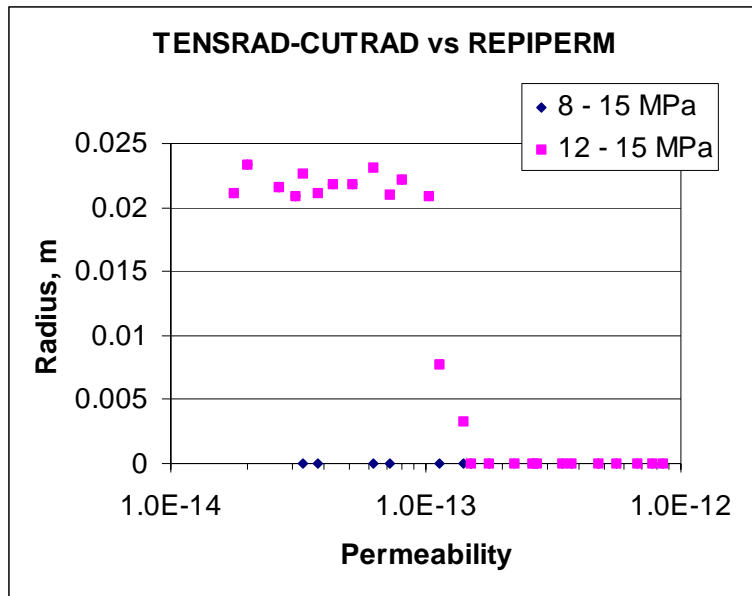


Figure 3-20. Scatterplot of TENS RAD-CUTRAD vs. REPIPERM for all 60 vectors.

## 4 RESULTS AND DISCUSSION – CYLINDRICAL GEOMETRY

In a real three-dimensional system, the drilling process creates a cylindrical borehole through the waste repository that constantly increases in length and possibly grows radially due to caving and spalling processes. To rigorously simulate a borehole that grows axially, radially, or both, under isotropic homogenous conditions would require a large, computationally-intensive two-dimensional axial-symmetric model. The probabilistic framework in which the spallings model is applied requires many executions, resulting in a necessary balance between model sophistication and computational efficiency. Development of a one-dimensional model geometry was seen as a strategy that would promote computational speed but still include all of the critical mechanisms proposed in the conceptual model. Therefore, two one-dimensional geometric models (hemispherical, cylindrical) are implemented in DRSPALL, with the geometry selected by the user. At early time just prior to and just after penetration, the repository domain is best modeled with hemispherical flow and stress state assumptions. As the bit approaches the floor of the repository the one-dimensional cylindrical assumption is more appropriate. In spite of this, only one geometry may be used per execution in the current DRSPALL model. The purpose of this discussion is to compare the results of cylindrical versus spherical repository geometry for the same set of input parameters.

### 4.1 Cylindrical vs. Spherical Geometry

The effect of the geometry on specific model setup parameters is demonstrated in Figure 4-1, which compares equivalent radius and enclosed volume for the two geometries as a function of drill bit penetration depth. Recall that the equivalence to the actual wellbore geometry drilled into the repository assumes conservation of cavity surface area (§ 2.3.1.1). The result is that neither the drilled radius nor the drilled volume is conserved. Surface area is conserved to provide consistency in the coupling of the wellbore and repository models with respect to gas flow. At early times for cylindrical geometry, the wellbore cavity is modeled as a very small diameter cylinder with a length equal to the repository height. As drilling proceeds, the actual 3-D wellbore cavity in the repository increases while radius remains constant. In the one-dimensional DRSPALL model, however, the wellbore cavity length is fixed and the radius increases to conserve surface area. When the drill bit reaches the repository floor at a depth of 1.5 m, the radius and volume for cylindrical geometry is slightly larger than the actual 3-D wellbore because the circular surface area at the bottom of the wellbore is included in the circumferential surface area of the cylindrical geometry model. In spherical geometry the equivalent radius and volume are considerably larger than that of the actual 3-D wellbore cavity. Recall that a sphere has the largest ratio of volume to surface area of any geometric shape, so for a given surface area, the volume of a hemisphere will be larger than that of a cylinder.

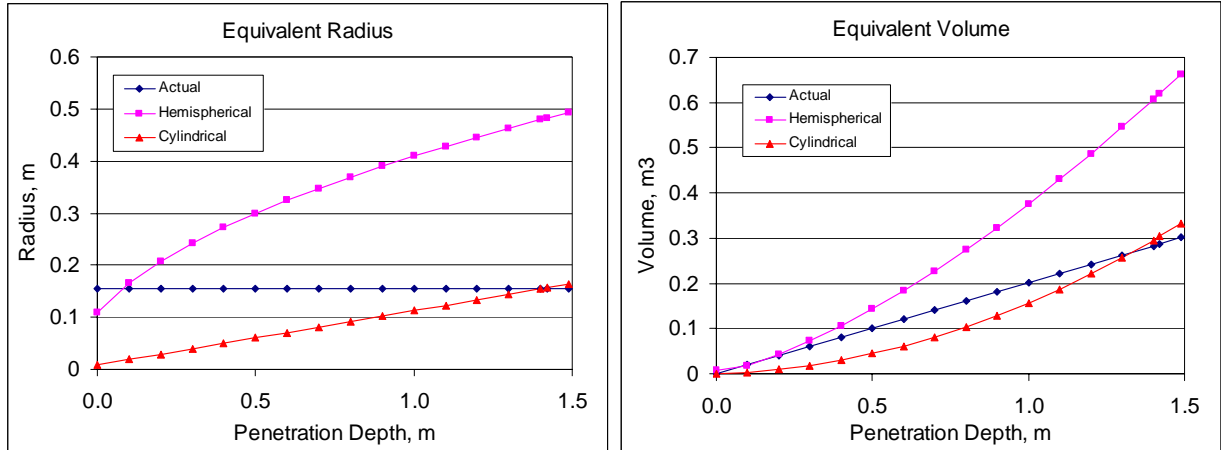


Figure 4-1. Equivalent radius and volume for one-dimensional hemispherical and cylindrical geometries

Figure 4-2 shows the effect of geometry on the radial elastic stress. Recall that the radial elastic stress ( $\sigma_{er}(r)$ ) represents the stress distribution as a function of radius  $r$  in a thick-walled shell, determined by the geometry and the boundary conditions. The formula used in DRSPALL (WIPP PA, 2003) appears as:

$$\sigma_{er}(r) = \left\{ \sigma_{ff} \left[ 1 - \left( \frac{r_c}{r} \right)^m \right] + p_c \left( \frac{r_c}{r} \right)^m \right\} \quad (4.1)$$

where  $\sigma_{ff}$  is the far-field stress outer boundary condition,  $r_c$  is the cavity (inner wall) radius,  $m$  is the geometry exponent (cyl:  $m = 2$ , sph:  $m = 3$ ), and  $p_c$  is the cavity pressure inner boundary condition. A spreadsheet was used to calculate stress profiles using Eq. 4.1 and the boundary conditions corresponding to a bit penetration depth of 0.7, with the resulting profiles shown in Figure 4-2. Three curves are shown: (1) cylindrical geometry with  $r_c = 0.082\text{m}$ , (2) hemispherical geometry with  $r_c = 0.35\text{ m}$ , and (3) cylindrical geometry with  $r_c = 0.35\text{ m}$ .

There are two major factors contributing to the differences in the stress profiles. One factor arises from the conservation of cavity surface area during drilling, which results in a much smaller equivalent cavity radius in cylindrical geometry ( $r_c = 0.082\text{m}$ ) versus spherical geometry ( $r_c = 0.35\text{m}$ ) at a given bit penetration depth. The inner boundaries in curves 1 and 2 correspond to the respective equivalent cavity radii for a real bit penetration depth of 0.7m. This smaller equivalent cavity radius results in larger compressive radial elastic stresses and a steeper stress gradient near the wellbore than in the spherical geometry. The other factor is the geometry. For the same cavity radius (compare curves 2 and 3 with  $R_c = 0.35\text{m}$ ), the cylindrical geometry has lower compressive stresses and gradients near the wellbore than the spherical (compare curves). The differing radius case (curve 1 vs. 2) is representative of the sensitivity results presented in § 4.2. The effect of these differences on effective stress and tensile failure

will be dependent on the pore pressure profile, which is a function of both geometry and time.

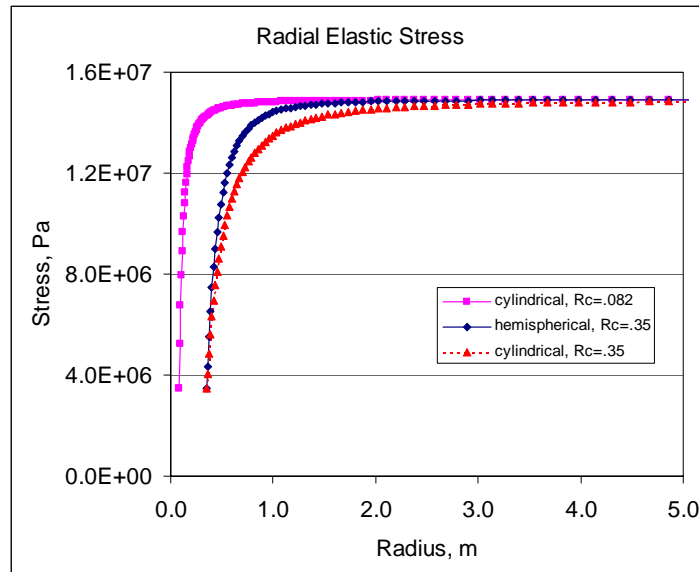


Figure 4-2. Radial elastic stress profiles for one-dimensional hemispherical and cylindrical geometries

For the discussions in the remainder of this section, the two sets of 30 runs used in the original sensitivity study presented in Section 3 were repeated with only the geometry input flag switched from hemispherical to cylindrical. All other sampled and numerical modeling parameters remained the same. The result was that zero spall release was calculated for all 60 vectors when using cylindrical geometry as compared to 4 vectors that had nonzero spall release when using spherical geometry (1 for 8-15MPa set and 3 for the 12-15MPa set). The summary of releases comparing the geometries for the 30 high pressure (12-15 MPa) runs is shown in Table 4-1.

Table 4-1. Summary of equivalent uncompacted spall volumes ( $m^3$ ) calculated for the 12-15 MPa sensitivity runs for spherical and cylindrical geometries.

Vector	SPLVOLEQ (12-15 MPa)		Vector	SPLVOLEQ (12-15 MPa)	
	Spherical	Cylindrical		Spherical	Cylindrical
20	1.2026	0	14	0	0
7	0.49153	0	16	0	0
15	0.049454	0	17	0	0
1	0	0	18	0	0
2	0	0	19	0	0
3	0	0	21	0	0
4	0	0	22	0	0
5	0	0	23	0	0
6	0	0	24	0	0
8	0	0	25	0	0
9	0	0	26	0	0
10	0	0	27	0	0
11	0	0	28	0	0
12	0	0	29	0	0
13	0	0	30	0	0

The effect of the geometry is demonstrated below in section 4.1 by comparing histories (variable versus time) and profiles (variable versus repository radius) of intermediate results for vector 020 from the high-pressure sampled set, which had the largest spall release in the original sensitivity study.

## 4.2 Vector 020 cylindrical vs. spherical results

In this section histories and profiles of intermediate results are compared to demonstrate the effect of the one-dimensional model geometries. Profiles were taken at 160 seconds or just after tensile failure began with spherical geometry. Note these profiles will have almost the same cavity surface area but different repository inner radii and drilled volumes because of the equivalent geometry assumption that conserves surface area.

### 4.2.1 History variables

Figure 4-3 shows bottomhole (BOTPRS) and cavity (CAVPRS) pressure histories for (a) the spherical geometry, and (b) the cylindrical geometry. Differences first appear at runtime ~20 sec, or 10 sec prior to bit penetration. While in the spherical geometry, cavity pressure at the face of the waste decreases from 14 to 10 MPa right before penetration, in cylindrical geometry, the cavity pressure decreases to ~13.5 MPa right before penetration. This implies that the pore pressure near point of penetration is higher in the cylindrical case than in the spherical case, and the pressure gradients will be lower at the time of intrusion. Consequently, the wellbore in the cylindrical case sees a much higher repository pressure upon penetration. Eventually, bottomhole pressure stabilizes at a lower value with the cylindrical repository geometry after 300 seconds. The spikes in pressure between 150 and 250s for the hemispherical case are due to fluidized waste entering the wellbore.

The difference in bottom hole pressure just prior to penetration is due to the wellbore numerical diffusion implementation at the bottom of the wellbore. The effect is amplified in the cylindrical case because of the smaller timesteps and smaller equivalent cavity radius relative to the spherical runs. Subsequent adjustments to the diffusion model have shown marked improvement in comparisons of early time bottom hole pressure. The effect of these adjustments on the spherical case was less significant and tended to reduce spall. These modifications will be incorporated in the results presented in the Sensitivity Analysis Report - Part II.

Figure 4-4 shows equivalent uncompacted spall (SPLVOLEQ), cuttings (CUTVOLEQ) and total (TOTVOLEQ) volume histories and clearly reveals the spall releases in the hemispherical case ( $1.2 \text{ m}^3$  at 900 seconds). Also evident is the difference in cuttings volume (final spherical CUTVOLEQ =  $0.66 \text{ m}^3$ , cylindrical CUTVOLEQ =  $0.33 \text{ m}^3$ ) because the equivalent geometries do not conserve volume. Similar results are shown for cavity radius (CAVRAD), tensile failure radius (TENS RAD) and equivalent drilling radius (DRILLRAD) in Figure 4-5. The fact that CAVRAD and TENS RAD overlay in Figure 4-4a after 150 seconds indicates that any solid material that failed in tension was also fluidized.

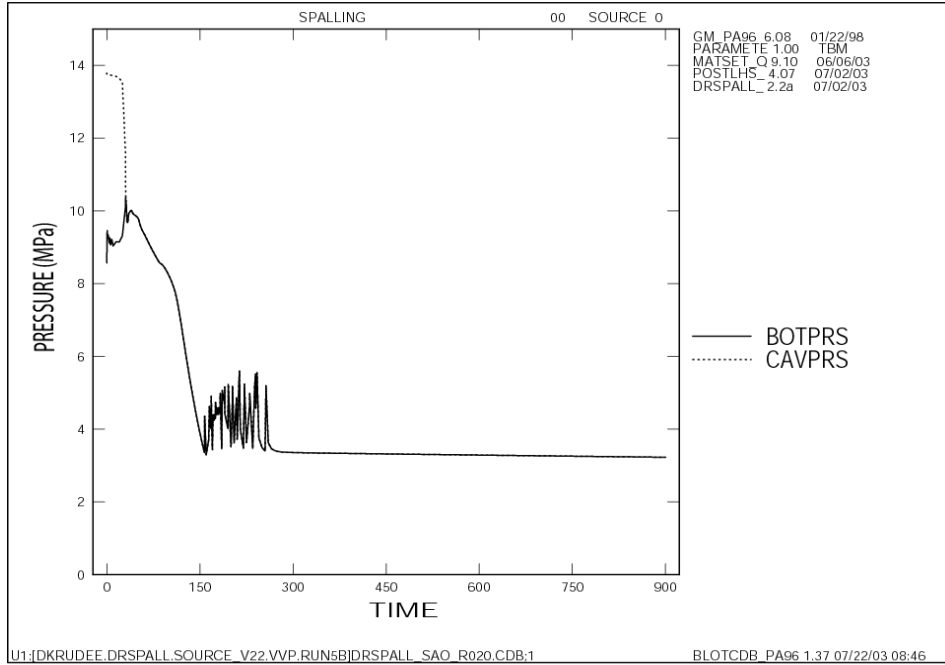
Figure 4-6 shows fluidization velocity threshold (FLUIDVEL) and superficial pore velocity (WBSUPVEL) histories for the cell next to the wellbore. The cell comprising the cavity wall varies as material is drilled or fails and fluidizes. Visible in the cylindrical geometry is the lower pore velocity at the time of penetration as a result of the lower pressure gradient. Late time pore velocity is higher in the cylindrical case because the wellbore interface is at a smaller radius (smaller flux area) due to no spall. In both geometries superficial gas velocity near the cavity face exceeded the fluidization threshold, indicating that for the spherical case, spall release was limited by cessation of failure rather than by the fluidization mechanism.

#### **4.2.2 Spatial variables**

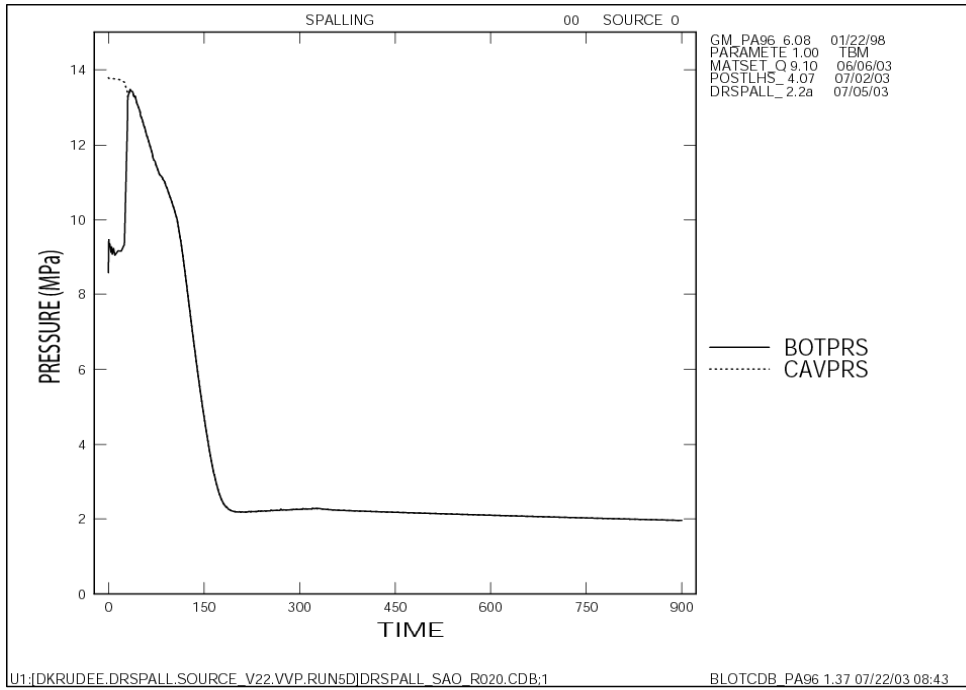
Figure 4-7 shows pore pressure (POREPRS) and radial total elastic stress (RADELSTR) profiles at 160 sec or just after the initial tensile failure. The effect of the geometry on gradients is apparent in pore pressure profiles, with the spherical case showing steeper gradients near the wellbore. This would also be expected in the elastic stress profile, however, the very small effective radius in the cylindrical geometry is strongly influencing the behavior near the well as was demonstrated earlier.

Figure 4-8 shows radial effective stress (RADEFSTR) and radial seepage stress (RADSPSTR) profiles over the entire repository domain at 160s. Figures 4-9 and 4-10 zoom in on radial effective stress in the region near the cavity wall where the tensile phase develops. Note that on these last two figures the abscissa is relative to the wall rather than the center axis of the wellbore. Also, recall that radial effective stress is calculated from the elastic stress minus the pore pressure (Figure 4-7) plus the seepage

stress and that its average value (over a characteristic length= 2.0 cm for this study) is compared to the tensile cutoff value to determine material failure. Therefore, its behavior is important in determining the effect of geometry on spall release. The seepage stress component is very similar for both geometries, indicating that the combined effects of geometry and differential pressure are similar in the two geometries. The peak compressive radial effective stress, however, is more than twice as large in the cylindrical case indicating the pore pressure has dropped more in the interior of the repository relative to the elastic stress. This is also evident in Figure 4-7. Close examination of the region near the cavity interface shows that radial effective stress does not go into tension in cylindrical geometry. In contrast, in the spherical geometry the phasing and relative gradients of the stress components develops a tensile phase right at the cavity interface that covers 2.2 cm and 9 zones. It is in this region that the average tensile stress will eventually exceed the tensile limit and cause failure.

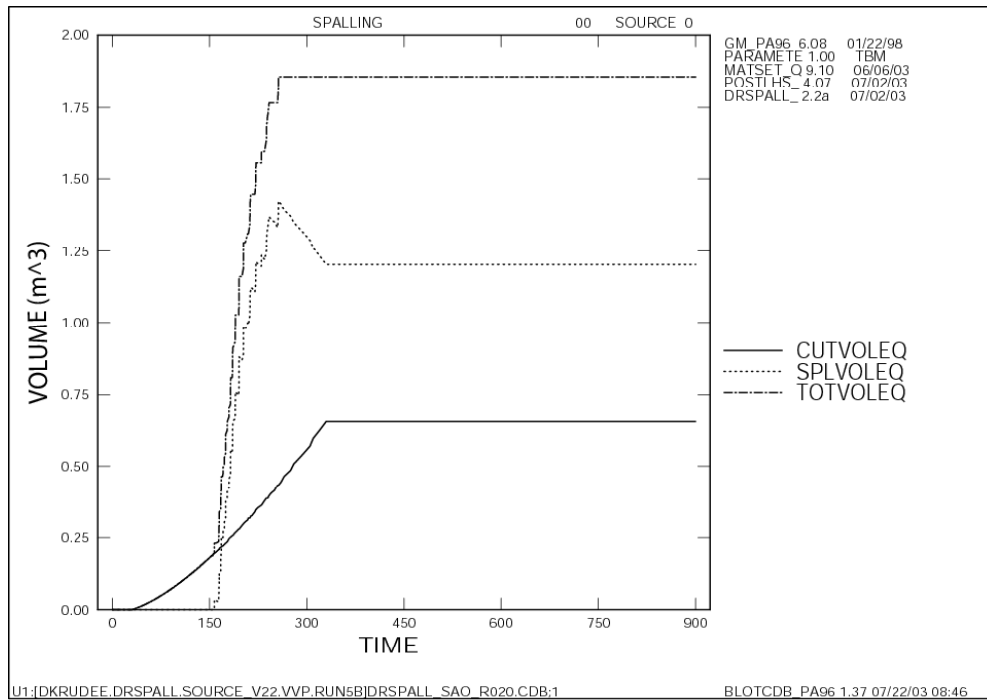


(a) Hemispherical

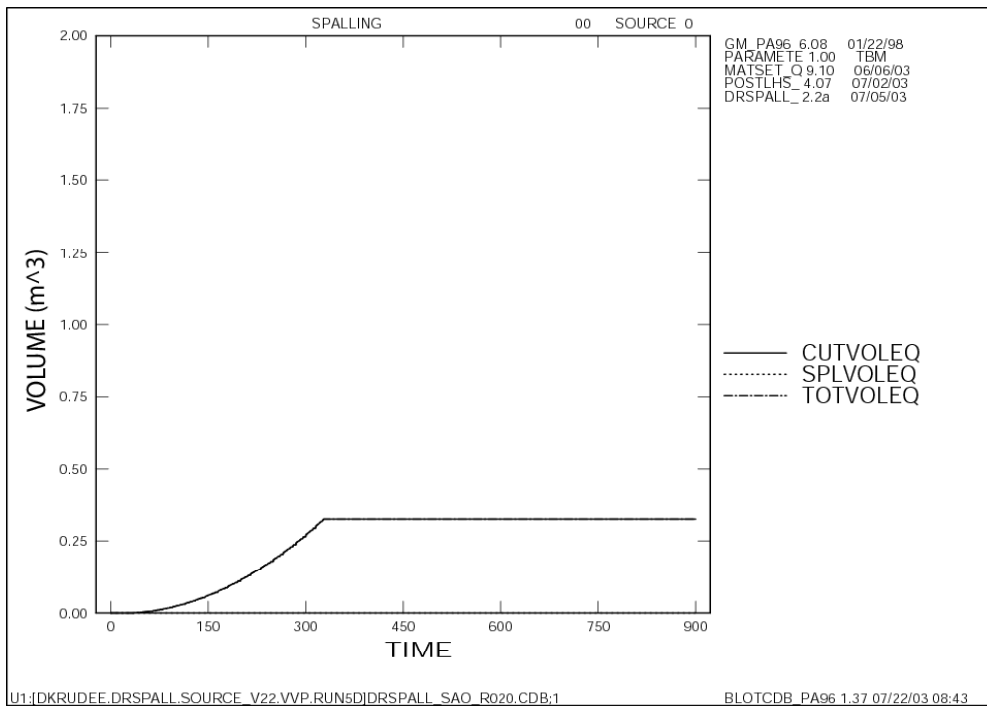


(b) Cylindrical

Figure 4-3. Bottomhole and cavity pressure histories

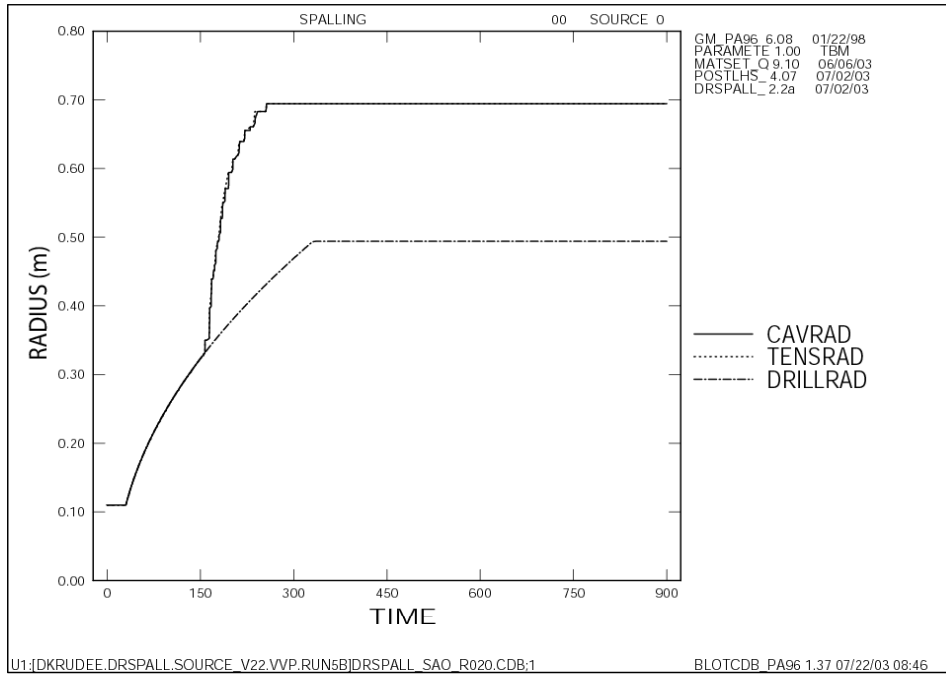


(a) Hemispherical

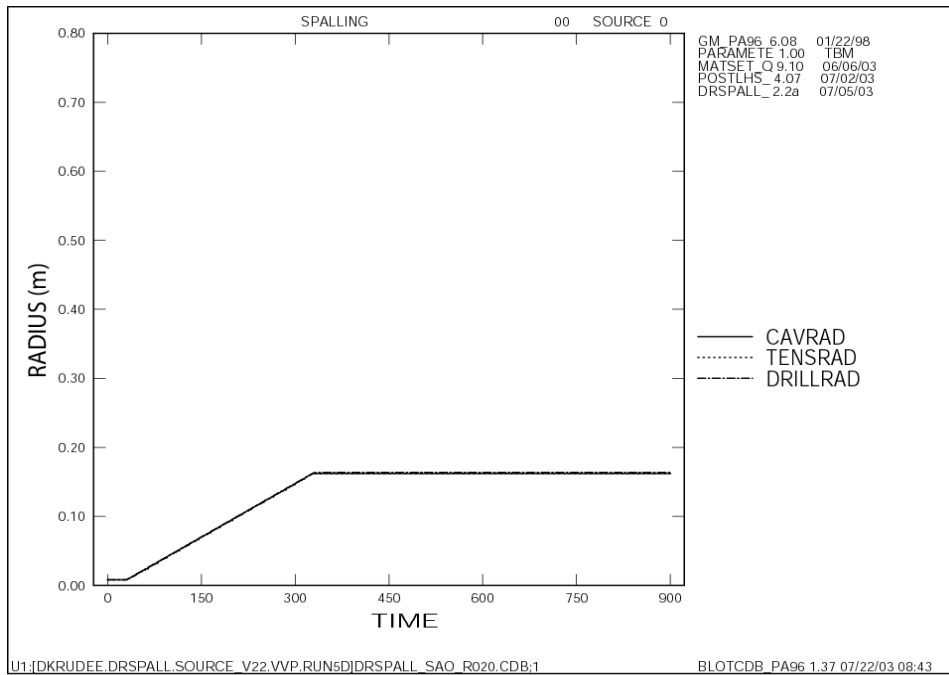


(b) Cylindrical

Figure 4-4. Cuttings, spall and total equivalent uncompacted volume histories

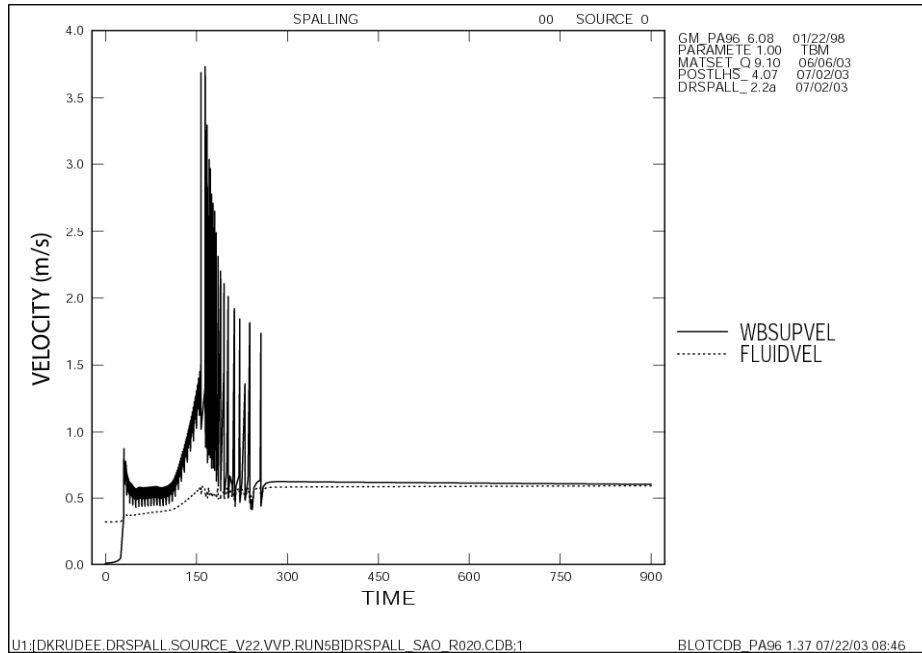


(a) Hemispherical

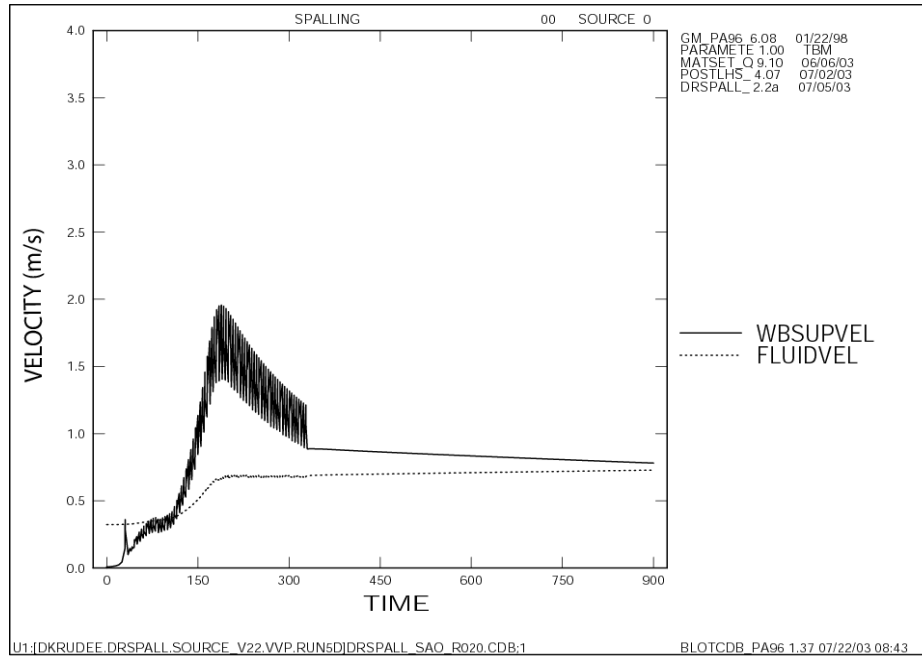


(b) Cylindrical

Figure 4-5. Cavity, tensile and equivalent drilling radii histories

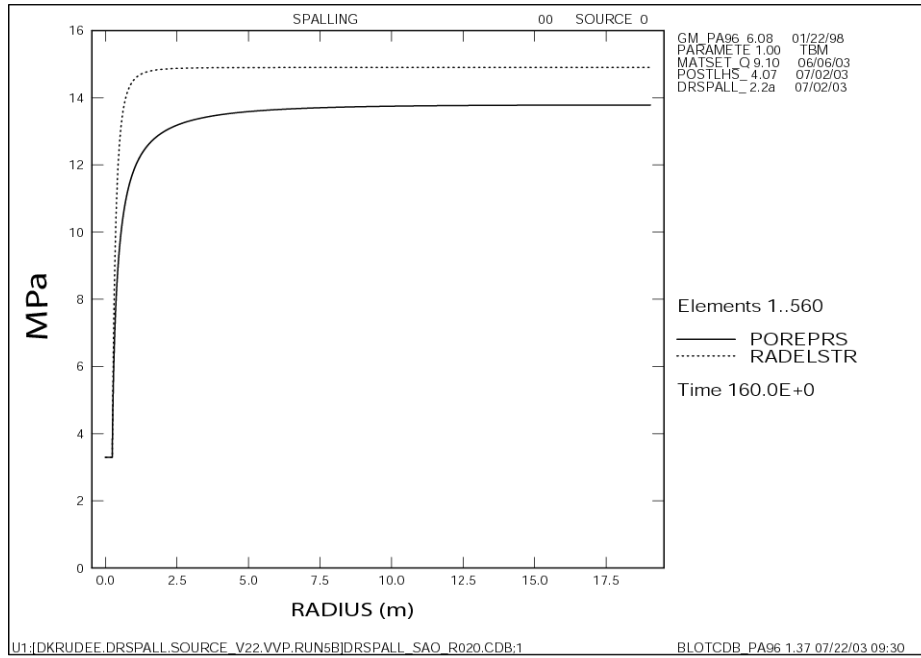


(a) Hemispherical

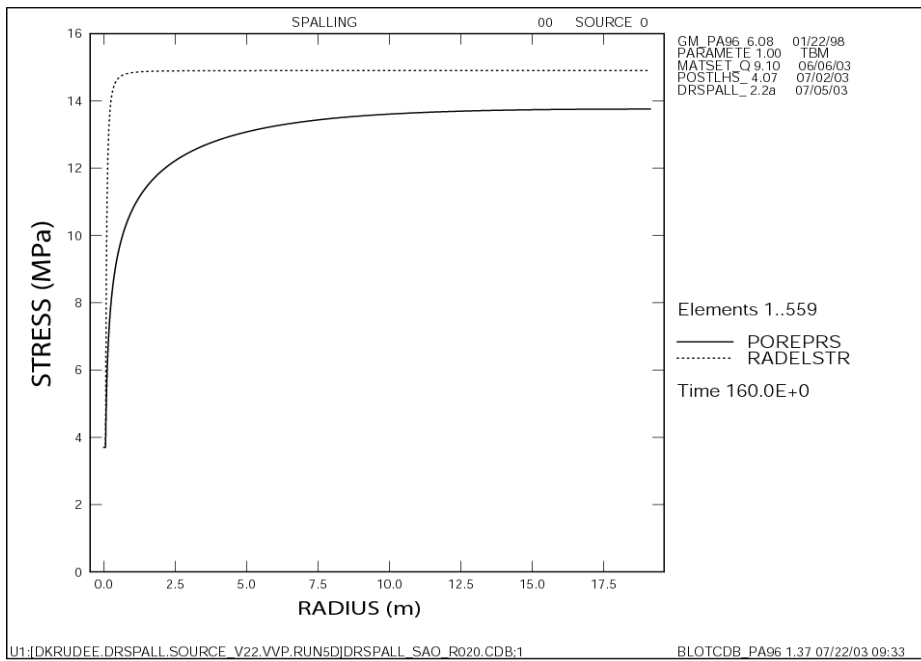


(b) Cylindrical

Figure 4-6. Fluidization threshold and superficial pore velocity histories

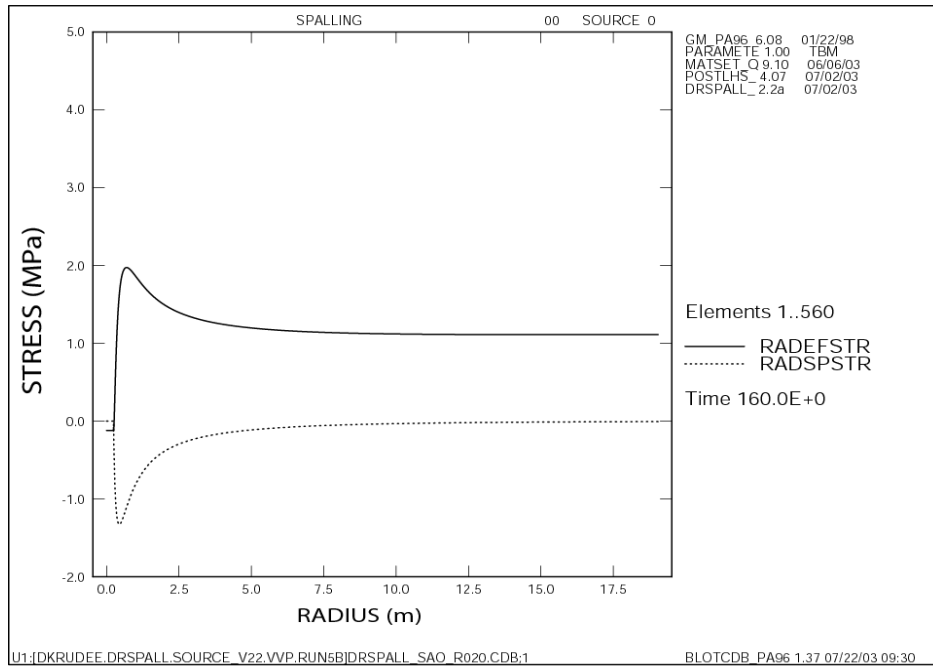


(a) Hemispherical

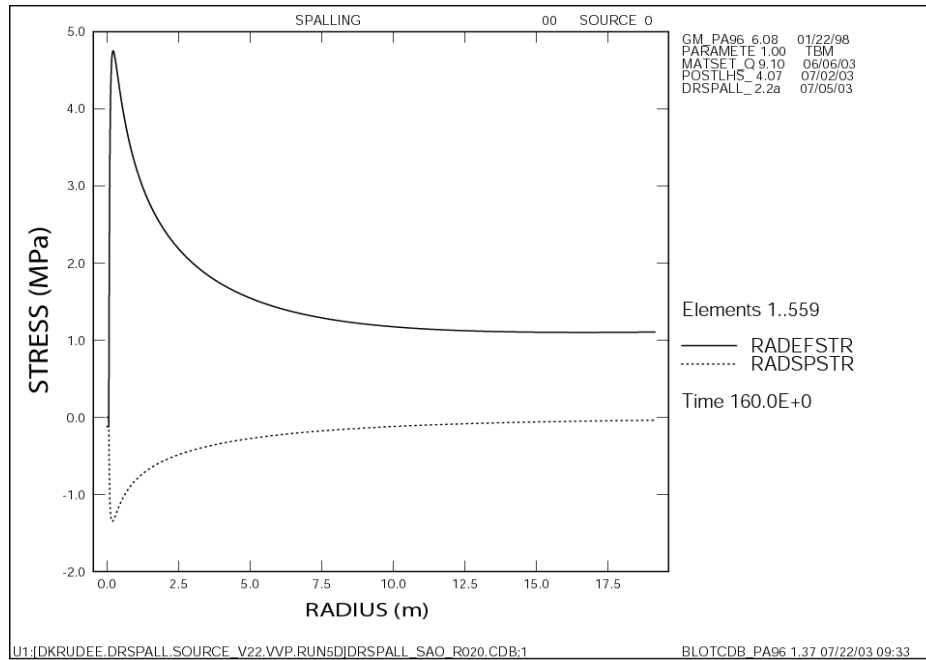


(b) Cylindrical

Figure 4-7. Pore pressure and radial elastic (total) stress profiles for entire repository domain.

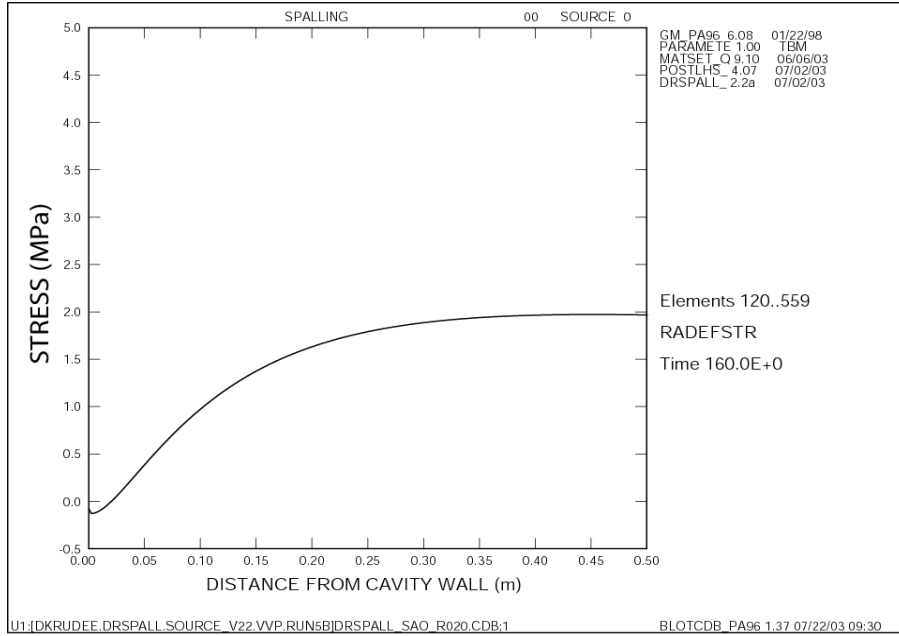


(a) Hemispherical

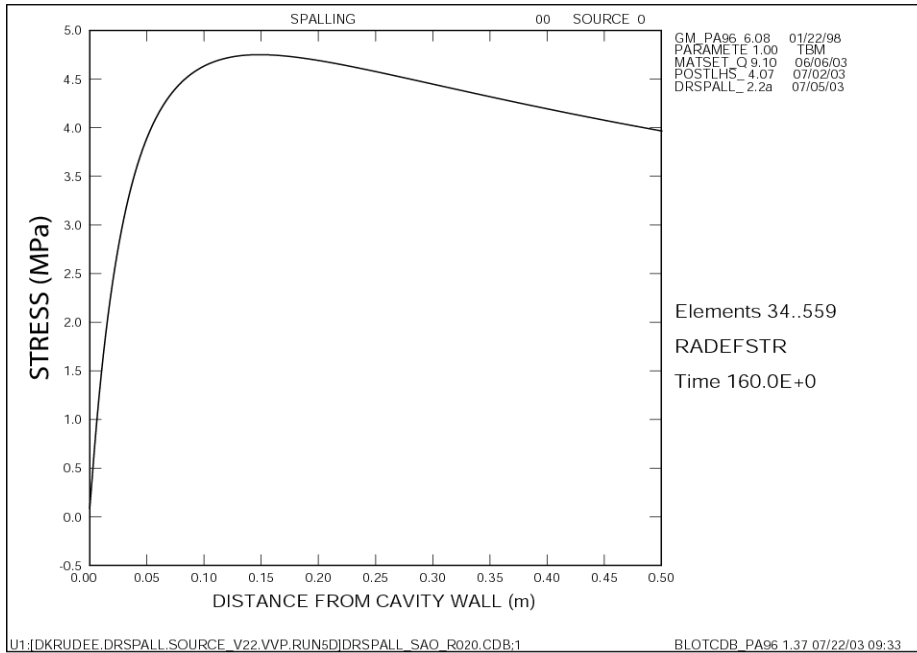


(b) Cylindrical

Figure 4-8. Radial effective and seepage stress profiles for entire repository domain.

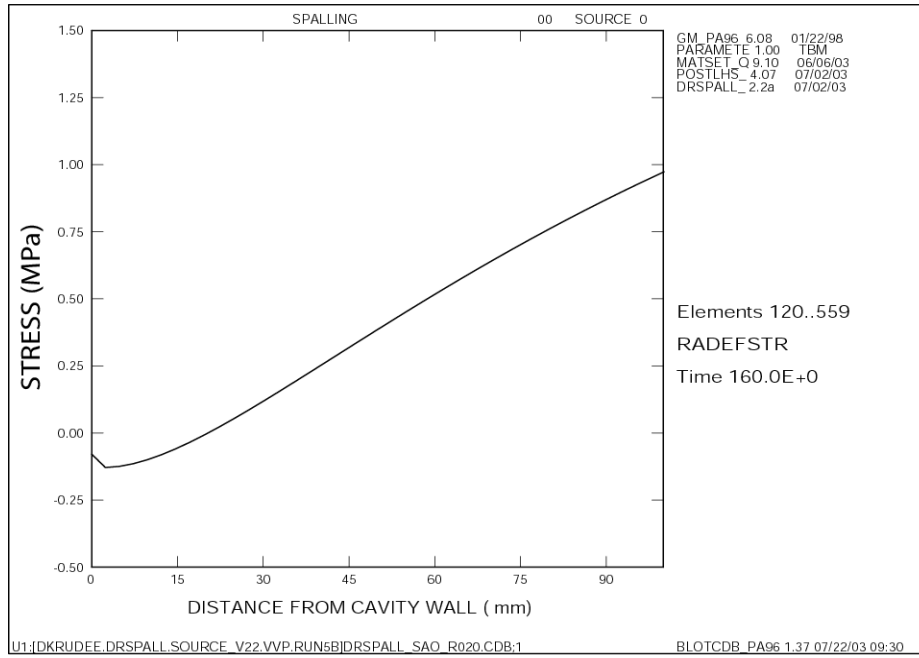


(a) Hemispherical

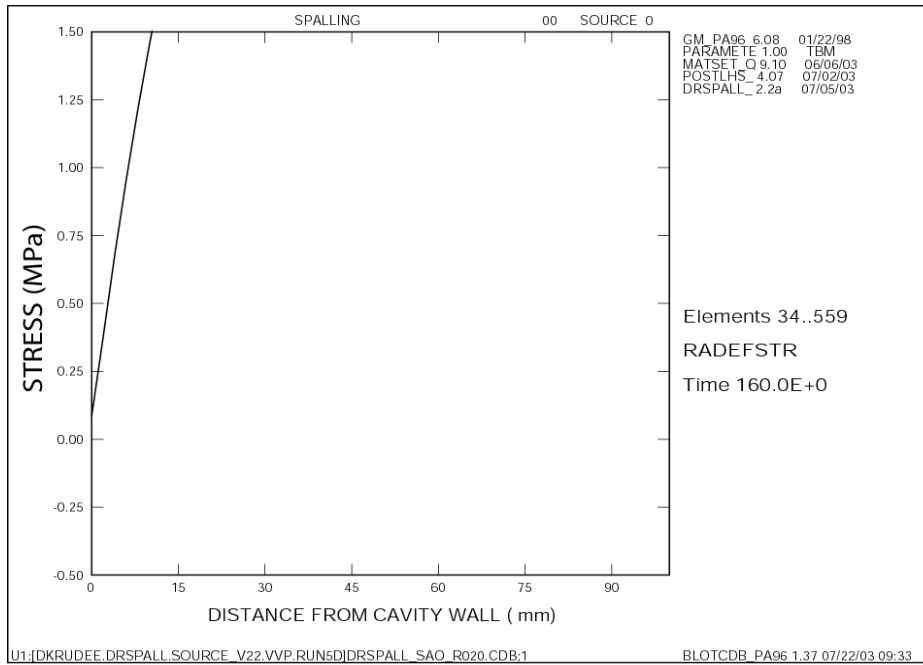


(b) Cylindrical

Figure 4-9. Radial effective stress profile (magnification 1)



(a) Hemispherical



(b) Cylindrical

Figure 4-10. Radial effective stress profile (magnification 2)

## 5 SUMMARY

The sensitivity analysis presented here indicates that the DRSPALL model shows a sensitivity to input parameters that is consistent with the conceptual model. Key parameters include repository pressure and repository permeability. Both of these factors are expected to directly affect the magnitude of tensile stresses, and the fluidization capacity of the system, which will, in turn, affect spall release volumes. No particular correlation was observed between spall release volumes and waste tensile strength or particle diameter  $\times$  shape factor over the range of input values examined (see Table 2-1). Most of the release volumes were actually zero (see Tables 3-4 and 4-1). This implies that spall releases are expected only in a small region of the parameter space.

The results of this sensitivity analysis allow for the following specific conclusions.

1. Spall volumes resulting from the sampled input parameters given in Table 2-1 ranged from 0 to 1.2 m<sup>3</sup> equivalent uncompacted volume.
2. No tensile failure was observed for
  - a. REPIPRES < 11 MPa
  - b. REPIPERM > 2E-13 m<sup>2</sup>
3. No spall releases were observed for
  - a. REPIPRES < 12 MPa
  - b. Cylindrical geometry
4. No particular correlation of SPLVOLEQ was observed for
  - a. the product PARTDIAM\*SHAPEFAC
5. No correlation of SPLVOLEQ or TENS RAD-CUTRAD was observed for
  - a. TENSLSTR varied from 0.12 to 0.17 MPa
6. The selected one-dimensional geometry has a significant effect on the calculation of spall release due its affect on pressure and stress gradients.
7. Spherical geometry is more likely to result in spall release, and is thus conservative relative to releases for the study shown here

**REFERENCES**

- DOE (U.S. Department of Energy). 1996. *Title 40 CFR Part 191 Compliance Certification Application for the Waste Isolation Pilot Plant*. DOE/CAO-1996-2184. Carlsbad, NM: United States Department of Energy, Waste Isolation Pilot Plant, Carlsbad Area Office. Vols I-XXI.
- Ergun, S. 1952. Fluid Flow Through Packed Columns. *Chemical Engineering Progress*. 48: 89-94.
- Hansen, F.D., Pfeifle, T.W., Lord, D.L. 2003. *Parameter Justification Report for DRSPALL*. Carlsbad, NM: Sandia National Laboratories.
- Helton, J. Davis, F.L. 2002. *Latin Hypercube Sampling and the Propagation of Uncertainty in Analyses of Complex Systems*. SAND2001-0417. Albuquerque, NM: Sandia National Laboratories.
- WIPP PA (Performance Assessment). 1996a. *User's Manual for BLOTADB Version 1.37, Document Version 1.00*, WPO# 37501. Carlsbad, NM: Sandia National Laboratories.
- WIPP PA (Performance Assessment). 1996b. *User's Manual for SPLAT Version 1.02, Document Version 1.01*, WPO# 40960. Carlsbad, NM: Sandia National Laboratories.
- WIPP PA (Performance Assessment). 2003. *Design Document for DRSPALL version 1.00, Document Version 1.10*. ERMS# 529878. Carlsbad, NM: Sandia National Laboratories.

## APPENDIX DEFAULTS

	<i>Parameter</i>	<i>Units</i>	<i>Source</i>	<i>MATERIAL</i>	<i>PROPERTY</i>	<i>Distribution</i>	<i>Median</i>	<i>Low</i>	<i>High</i>
1	Land Elevation	m	NEW			Constant	1.037E+03		
2	Repository Top	m	NEW			Constant	3.847E+02		
3	DRZ Permeability	m2	CCA PA database	DRZ_1	PRMX_LOG	LogUniform	1.122E-16	3.981E-20	3.162E-13
4	Initial Gas Pressure	Pa	BRAGFLO			Uniform	1.145E+07	8.000E+06	1.490E+07
5	Far-Field In-Situ Stress	Pa	NEW			Constant	1.490E+07		
6	Porosity	-	BRAGFLO			Uniform	5.050E-01	3.500E-01	6.600E-01
7	Permeability	m2	NEW RANGE			LogUniform	2.400E-13	2.400E-14	2.400E-12
8	Biot Beta	--	NEW			Constant	1.000E+00		
9	Poisson's Ratio	--	NEW			Uniform	3.900E-01	3.500E-01	4.300E-01
10	Cohesion	Pa	NEW			Constant	1.400E+05		
11	Friction Angle	deg	NEW			Constant	4.580E+01		
12	Tensile Strength	Pa	NEW VALUE			Uniform	1.450E+05	1.200E+05	1.700E+05
13	Particle Diameter	m	NEW			LogUniform	1.000E-02	1.000E-03	1.000E-01
14	Gas Viscosity	Pa*s	CCA PA database	H2	VISCO	Constant	8.934E-06		
15	Mud Density	kg/m3	CCA PA database	DRILLMUD	DNSFLUID	Cumulative	1.210E+03	1.140E+03	1.380E+03
16	Mud Viscosity	Pa*s	CCA PA database	DRILLMUD	VISCO	Cumulative	1.100E-02	5.000E-03	3.000E-02
17	Pipe roughness	m	NEW			Constant	5.000E-05		
18	Wellbore roughness	m	NEW			Loguniform	3.937E-04	5.000E-05	3.100E-03
19	Max. Solids Vol. Fraction	--	NEW			Uniform	6.150E-01	5.900E-01	6.400E-01
20	Solids Viscosity Exponent	--	NEW			Uniform	-1.500E+00	-1.800E+00	-1.200E+00
21	Bit Diameter	m	CCA PA database	BOREHOLE	DIAMMOD	Constant	3.112E-01		
22	Pipe Diameter	m	CCA PA database	BOREHOLE	PIPED	Constant	1.143E-01		
23	Collar Diameter	m	CCA PA database	BOREHOLE	COLDIA	Constant	2.032E-01		
24	Pipe Inside Diameter	m	NEW			Constant	9.718E-02		
25	Collar Length	m	CCA PA database	BOREHOLE	L1	Constant	1.829E+02		
26	Drilling Rate	m/s	NEW			Uniform	4.445E-03	2.963E-03	5.927E-03
27	Mud Pump Rate	m3/s	NEW			Uniform	2.018E-02	1.615E-02	2.422E-02
28	DDZ Thickness	m	NEW			Constant	1.600E-01		
29	DDZ Permeability	m2	NEW			LogUniform	1.000E-14	1.000E-15	1.000E-13

30	Stop Drilling Exit Vol Rate	m3/s	NEW			Constant	1.000E+03		
31	Stop Pumping Exit Vol rate	m3/s	NEW			Constant	1.000E+03		
32	$\pi$	-	CCA PA database	REFCON	PI	Constant	3.142E+00		
33	Atmospheric pressure	Pa	NEW			Constant	1.017E+05		
34	Gravitational constant	m/s <sup>2</sup>	CCA PA database	REFCON	GRAVACC	Constant	9.807E+00		
35	Water Compressibility	1/Pa	CCA PA database	BRINESAL	COMPRES	Constant	3.100E-10		
36	Gas Constant	J/kg K	CCA PA database	BLOWOUT	RGAS	Constant	4.116E+03		
37	Repository Temperature	K	CCA PA database	BLOWOUT	TREPO	Constant	3.000E+02		
38	Waste Density	kg/m <sup>3</sup>	CCA PA database	BLOWOUT	RHOS	Constant	2.650E+03		
39	Salt Density	kg/m <sup>3</sup>	NEW			Constant	2.180E+03		
40	Shape Factor	--	NEW			Uniform	5.500E-01	1.000E-01	1.000E+00
41	Bit Nozzle Number	--	NEW			Constant	3.000E+00		
42	Bit Nozzle Diameter	m	NEW			Constant	1.111E-02		

**APPENDIX LHS2\_DRSPALL.TRN**

The following is a listing of the ASCII output file LHS2\_DRSPALL.TRN created by running LHS. Also created are 30 output binary files (1 per vector) that are not listed here. Note that the sampled parameter names, distributions, and ranges are given on the first page of this listing. Below this appears a table of the new parameter values computed by LHS, followed by a similar table showing the rank of a particular value within the distribution of 30 values. Rank = 1 corresponds to the lowest value in the distribution, while rank = 30 corresponds to the highest value. The final collection of tables show the histograms for each sampled variable.

U1:[DKRUDEE.DRSPALL.LHSJUL1]LHS2\_DRSPALL.TRN;36  
 1-JUL-2003 19:15:52.72

```

1
    TITLE DRSPALL SENSITIVITY SAMPLING

    RANDOM SEED =    585364674

    NUMBER OF VARIABLES =  15

    NUMBER OF OBSERVATIONS =   30
0   THE SAMPLE INPUT VECTORS WILL BE PRINTED ALONG WITH THEIR CORRESPONDING RANKS
0   HISTOGRAMS OF THE ACTUAL SAMPLE WILL BE PLOTTED FOR EACH INPUT VARIABLE
0   THE CORRELATION MATRICES (RAW DATA AND RANK CORRELATIONS) WILL BE PRINTED
1
    
```

```

    TITLE DRSPALL SENSITIVITY SAMPLING
    
```

VARIABLE	DISTRIBUTION	RANGE	LABEL
0 1	UNIFORM	8.0000E+06 TO 1.4850E+07	DR_SPALL REPIPRES
0 2	UNIFORM	0.3500 TO 0.6600	DR_SPALL REPIPOR
0 3	LOGUNIFORM	1.7000E-14 TO 1.7000E-12	DR_SPALL REPIPERM
0 4	UNIFORM	0.3500 TO 0.4300	DR_SPALL POISRAT
0 5	LOGUNIFORM	1.2000E+05 TO 1.7000E+05	DR_SPALL TENSLSSTR
0 6	UNIFORM	1140. TO 1380.	DR_SPALL INITMDEN
0 7	UNIFORM	5.0000E-03 TO 3.0000E-02	DR_SPALL MUDVISCO
0 8	UNIFORM	0.5900 TO 0.6400	DR_SPALL MUDSOLMX
0 9	UNIFORM	-1.800 TO -1.200	DR_SPALL MUDSOLVE
0 10	UNIFORM	2.9600E-03 TO 5.9300E-03	DR_SPALL DRILRATE
0 11	UNIFORM	1.6100E-02 TO 2.4200E-02	DR_SPALL MUDPRATE
0 12	LOGUNIFORM	1.0000E-15 TO 1.0000E-13	DR_SPALL DDZPERM
0 13	LOGUNIFORM	5.0000E-05 TO 3.1000E-03	DR_SPALL WALLROUG

```

0      14      UNIFORM          0.1000      TO      1.000      DR_SPALL SHAPEFAC
0      15      UNIFORM          1.0000E-03 TO      1.0000E-02 DR_SPALL PARTDIAM
1TITLE DRSPALL SENSITIVITY SAMPLING
0LATIN HYPERCUBE SAMPLE INPUT VECTORS
    
```

RUN NO.	X(1)	X(2)	X(3)	X(4)	X(5)	X(6)	X(7)	X(8)	X(9)	X(10)	
0	1	1.438E+07	5.384E-01	1.049E-12	4.112E-01	1.304E+05	1.290E+03	1.859E-02	6.280E-01	-1.655E+00	3.282E-03
0	2	1.117E+07	5.965E-01	6.201E-14	3.997E-01	1.432E+05	1.257E+03	1.556E-02	6.002E-01	-1.770E+00	5.637E-03
0	3	1.184E+07	5.643E-01	8.527E-13	3.572E-01	1.483E+05	1.216E+03	2.526E-02	5.966E-01	-1.671E+00	4.104E-03
0	4	1.035E+07	6.092E-01	7.705E-13	3.819E-01	1.666E+05	1.318E+03	8.659E-03	6.185E-01	-1.711E+00	5.839E-03
0	5	9.268E+06	4.999E-01	2.722E-13	4.166E-01	1.247E+05	1.312E+03	9.751E-03	6.096E-01	-1.261E+00	4.039E-03
0	6	1.456E+07	6.346E-01	3.413E-13	3.829E-01	1.269E+05	1.372E+03	2.805E-02	5.930E-01	-1.389E+00	4.540E-03
0	7	1.389E+07	3.930E-01	1.133E-13	4.188E-01	1.599E+05	1.273E+03	1.931E-02	6.340E-01	-1.539E+00	5.179E-03
0	8	1.464E+07	4.528E-01	3.733E-13	3.849E-01	1.445E+05	1.196E+03	1.463E-02	6.399E-01	-1.443E+00	5.626E-03
0	9	1.257E+07	5.682E-01	8.004E-14	4.034E-01	1.521E+05	1.247E+03	1.238E-02	6.292E-01	-1.357E+00	3.013E-03
0	10	9.421E+06	3.748E-01	5.597E-13	4.225E-01	1.349E+05	1.349E+03	8.264E-03	6.059E-01	-1.788E+00	3.563E-03
0	11	8.232E+06	4.335E-01	2.608E-13	4.293E-01	1.232E+05	1.204E+03	2.739E-02	6.367E-01	-1.686E+00	5.120E-03
0	12	1.343E+07	4.653E-01	1.188E-12	3.642E-01	1.423E+05	1.227E+03	1.615E-02	6.311E-01	-1.607E+00	3.161E-03
0	13	1.160E+07	5.522E-01	5.154E-14	3.590E-01	1.689E+05	1.335E+03	1.359E-02	6.210E-01	-1.496E+00	5.242E-03
0	14	1.081E+07	4.597E-01	3.293E-14	4.077E-01	1.631E+05	1.263E+03	1.151E-02	5.986E-01	-1.232E+00	3.502E-03
0	15	1.017E+07	3.686E-01	1.510E-13	3.512E-01	1.320E+05	1.284E+03	1.833E-02	6.266E-01	-1.426E+00	4.192E-03
0	16	8.108E+06	4.931E-01	1.403E-13	3.536E-01	1.653E+05	1.306E+03	2.966E-02	6.222E-01	-1.544E+00	4.348E-03
0	17	1.401E+07	4.151E-01	2.660E-14	3.976E-01	1.552E+05	1.361E+03	1.318E-02	5.968E-01	-1.756E+00	3.067E-03
0	18	9.606E+06	3.593E-01	4.734E-13	3.720E-01	1.364E+05	1.366E+03	2.498E-02	6.321E-01	-1.256E+00	4.851E-03
0	19	1.053E+07	5.119E-01	2.238E-13	4.262E-01	1.542E+05	1.343E+03	2.608E-02	6.042E-01	-1.309E+00	5.342E-03
0	20	1.229E+07	6.013E-01	1.778E-13	3.703E-01	1.204E+05	1.324E+03	1.069E-02	6.123E-01	-1.208E+00	4.956E-03
0	21	1.309E+07	5.213E-01	3.077E-14	4.218E-01	1.613E+05	1.148E+03	2.374E-02	6.167E-01	-1.328E+00	4.582E-03
0	22	1.257E+07	5.343E-01	1.763E-14	3.914E-01	1.333E+05	1.176E+03	2.873E-02	6.172E-01	-1.508E+00	3.856E-03
0	23	9.963E+06	6.530E-01	3.765E-14	3.787E-01	1.295E+05	1.298E+03	2.232E-02	6.242E-01	-1.736E+00	3.725E-03
0	24	8.850E+06	6.266E-01	6.761E-13	4.120E-01	1.405E+05	1.242E+03	1.731E-02	6.134E-01	-1.281E+00	4.287E-03
0	25	8.486E+06	6.469E-01	7.238E-14	3.754E-01	1.465E+05	1.167E+03	5.231E-03	6.361E-01	-1.463E+00	3.808E-03
0	26	8.953E+06	4.049E-01	1.304E-12	3.875E-01	1.585E+05	1.148E+03	2.327E-02	5.909E-01	-1.571E+00	3.393E-03
0	27	1.122E+07	4.813E-01	1.996E-14	3.662E-01	1.220E+05	1.186E+03	2.130E-02	6.022E-01	-1.593E+00	5.472E-03
0	28	1.288E+07	3.828E-01	1.029E-13	3.620E-01	1.279E+05	1.189E+03	6.803E-03	6.115E-01	-1.628E+00	4.679E-03
0	29	1.353E+07	5.783E-01	1.498E-12	3.931E-01	1.501E+05	1.159E+03	2.051E-02	6.073E-01	-1.379E+00	4.808E-03
0	30	1.202E+07	4.280E-01	4.326E-14	4.029E-01	1.393E+05	1.235E+03	6.171E-03	5.944E-01	-1.404E+00	5.788E-03

```

1TITLE DRSPALL SENSITIVITY SAMPLING
0LATIN HYPERCUBE SAMPLE INPUT VECTORS
    
```

RUN NO.	X(11)	X(12)	X(13)	X(14)	X(15)	
0	1	2.198E-02	1.037E-15	4.283E-04	8.799E-01	7.877E-03
0	2	2.126E-02	4.275E-14	1.185E-03	9.946E-01	6.897E-03
0	3	1.773E-02	3.216E-14	1.607E-03	2.454E-01	8.133E-03
0	4	1.670E-02	2.083E-14	6.685E-05	2.012E-01	5.907E-03
0	5	1.763E-02	6.650E-15	2.601E-03	7.045E-01	4.510E-03
0	6	2.253E-02	5.619E-14	8.783E-05	5.017E-01	7.274E-03
0	7	2.096E-02	1.834E-15	1.529E-03	1.727E-01	8.766E-03

0	8	1.880E-02	7.667E-14	2.111E-03	5.325E-01	4.714E-03
0	9	1.741E-02	8.671E-14	5.510E-05	5.862E-01	6.605E-03
0	10	2.168E-02	2.872E-14	1.021E-04	1.077E-01	2.326E-03
0	11	2.284E-02	3.890E-14	1.275E-04	7.944E-01	3.523E-03
0	12	1.657E-02	1.903E-15	2.199E-04	9.413E-01	5.617E-03
0	13	2.362E-02	9.618E-15	5.954E-04	9.313E-01	2.976E-03
0	14	2.324E-02	4.794E-14	1.170E-03	8.925E-01	6.153E-03
0	15	2.204E-02	3.502E-15	1.979E-03	3.289E-01	3.217E-03
0	16	2.066E-02	4.995E-15	8.580E-05	6.764E-01	4.903E-03
0	17	2.110E-02	2.274E-15	7.877E-04	6.563E-01	2.617E-03
0	18	2.028E-02	6.865E-14	4.536E-04	5.761E-01	8.200E-03
0	19	1.633E-02	1.237E-15	2.990E-04	7.336E-01	5.262E-03
0	20	1.939E-02	3.162E-15	1.523E-04	2.932E-01	1.476E-03
0	21	2.003E-02	1.076E-14	3.647E-04	4.332E-01	1.055E-03
0	22	1.896E-02	2.821E-15	1.441E-04	1.498E-01	9.714E-03
0	23	1.910E-02	2.311E-14	3.088E-03	2.738E-01	4.145E-03
0	24	2.392E-02	1.425E-15	6.829E-04	6.339E-01	9.202E-03
0	25	1.968E-02	7.852E-15	5.391E-04	4.237E-01	7.361E-03
0	26	1.814E-02	1.595E-14	9.197E-04	4.839E-01	3.880E-03
0	27	1.696E-02	1.386E-14	1.834E-04	7.683E-01	1.851E-03
0	28	2.308E-02	4.129E-15	6.057E-05	8.454E-01	8.925E-03
0	29	2.419E-02	5.414E-15	2.289E-04	3.590E-01	2.130E-03
0	30	1.837E-02	1.331E-14	2.935E-04	3.820E-01	9.659E-03

1TITLE DRSPALL SENSITIVITY SAMPLING  
 0RANKS OF LATIN HYPERCUBE SAMPLE INPUT VECTORS

RUN NO.	X(1)	X(2)	X(3)	X(4)	X(5)	X(6)	X(7)	X(8)	X(9)	X(10)	
0	1	28.	19.	27.	23.	8.	19.	17.	23.	8.	4.
0	2	14.	24.	9.	19.	16.	15.	13.	7.	2.	28.
0	3	17.	21.	26.	3.	19.	10.	25.	4.	7.	12.
0	4	11.	26.	25.	12.	29.	23.	5.	18.	5.	30.
0	5	6.	15.	19.	25.	4.	22.	6.	12.	27.	11.
0	6	29.	28.	20.	13.	5.	30.	28.	2.	21.	16.
0	7	26.	5.	13.	26.	25.	17.	18.	27.	14.	23.
0	8	30.	10.	21.	14.	17.	8.	12.	30.	18.	27.
0	9	20.	22.	11.	21.	21.	14.	9.	24.	23.	1.
0	10	7.	3.	23.	28.	11.	27.	4.	10.	1.	7.
0	11	2.	9.	18.	30.	3.	9.	27.	29.	6.	22.
0	12	24.	12.	28.	6.	15.	11.	14.	25.	10.	3.
0	13	16.	20.	8.	4.	30.	25.	11.	19.	16.	24.
0	14	13.	11.	5.	22.	27.	16.	8.	6.	29.	6.
0	15	10.	2.	15.	1.	9.	18.	16.	22.	19.	13.
0	16	1.	14.	14.	2.	28.	21.	30.	20.	13.	15.
0	17	27.	7.	3.	18.	23.	28.	10.	5.	3.	2.
0	18	8.	1.	22.	9.	12.	29.	24.	26.	28.	20.
0	19	12.	16.	17.	29.	22.	26.	26.	9.	25.	25.
0	20	19.	25.	16.	8.	1.	24.	7.	14.	30.	21.

0	21	23.	17.	4.	27.	26.	2.	23.	16.	24.	17.
0	22	21.	18.	1.	16.	10.	5.	29.	17.	15.	10.
0	23	9.	30.	6.	11.	7.	20.	21.	21.	4.	8.
0	24	4.	27.	24.	24.	14.	13.	15.	15.	26.	14.
0	25	3.	29.	10.	10.	18.	4.	1.	28.	17.	9.
0	26	5.	6.	29.	15.	24.	1.	22.	1.	12.	5.
0	27	15.	13.	2.	7.	2.	6.	20.	8.	11.	26.
0	28	22.	4.	12.	5.	6.	7.	3.	13.	9.	18.
0	29	25.	23.	30.	17.	20.	3.	19.	11.	22.	19.
0	30	18.	8.	7.	20.	13.	12.	2.	3.	20.	29.

1TITILE DRSPALL SENSITIVITY SAMPLING  
0RANKS OF LATIN HYPERCUBE SAMPLE INPUT VECTORS

RUN NO.	X(11)	X(12)	X(13)	X(14)	X(15)	
0	1	22.	1.	16.	26.	23.
0	2	20.	25.	24.	30.	20.
0	3	7.	23.	26.	5.	24.
0	4	3.	20.	3.	4.	17.
0	5	6.	13.	29.	21.	12.
0	6	24.	27.	5.	14.	21.
0	7	18.	4.	25.	3.	26.
0	8	10.	29.	28.	15.	13.
0	9	5.	30.	1.	17.	19.
0	10	21.	22.	6.	1.	5.
0	11	25.	24.	7.	24.	9.
0	12	2.	5.	11.	29.	16.
0	13	28.	15.	19.	28.	7.
0	14	27.	26.	23.	27.	18.
0	15	23.	9.	27.	8.	8.
0	16	17.	11.	4.	20.	14.
0	17	19.	6.	21.	19.	6.
0	18	16.	28.	17.	16.	25.
0	19	1.	2.	14.	22.	15.
0	20	13.	8.	9.	7.	2.
0	21	15.	16.	15.	12.	1.
0	22	11.	7.	8.	2.	30.
0	23	12.	21.	30.	6.	11.
0	24	29.	3.	20.	18.	28.
0	25	14.	14.	18.	11.	22.
0	26	8.	19.	22.	13.	10.
0	27	4.	18.	10.	23.	3.
0	28	26.	10.	2.	25.	27.
0	29	30.	12.	12.	9.	4.
0	30	9.	17.	13.	10.	29.

1 TITLE DRSPALL SENSITIVITY SAMPLING  
0 HISTOGRAM FOR VARIABLE NO. 1 UNIFORM DISTRIBUTION

MIDPOINT	FREQ.	
8085000.	2	XX
8414999.	1	X
8744999.	1	X
9074999.	1	X
9404999.	2	XX
9734999.	1	X
0.1006500E+08	2	XX
0.1039500E+08	2	XX
0.1072500E+08	1	X
0.1105500E+08	2	XX
0.1138500E+08	0	
0.1171500E+08	2	XX
0.1204500E+08	1	X
0.1237500E+08	1	X
0.1270500E+08	2	XX
0.1303500E+08	2	XX
0.1336500E+08	2	XX
0.1369500E+08	0	
0.1402500E+08	2	XX
0.1435500E+08	1	X
0.1468500E+08	2	XX
0	30	

MIN	MAX	RANGE	MEAN	MEDIAN	VARIANCE
8107682.	0.1463851E+08	6530831.	0.1141358E+08	0.1140833E+08	0.3985014E+13

1 TITLE DRSPALL SENSITIVITY SAMPLING  
 0 HISTOGRAM FOR VARIABLE NO. 2 UNIFORM DISTRIBUTION

MIDPOINT	FREQ.	
0.3525000	1	X
0.3675000	2	XX
0.3825001	1	X
0.3975001	2	XX
0.4125001	1	X
0.4275001	2	XX
0.4425001	0	
0.4575001	2	XX
0.4725001	1	X
0.4875002	2	XX
0.5025002	1	X
0.5175002	2	XX

```

0.5325001      2  XX
0.5475001      1  X
0.5625001      2  XX
0.5775001      1  X
0.5925001      1  X
0.6075001      2  XX
0.6225001      1  X
0.6375000      1  X
0.6525000      2  XX
0
30
    
```

MIN	MAX	RANGE	MEAN	MEDIAN	VARIANCE
0.3592504	0.6529922	0.2937418	0.5049652	0.5059057	0.7999992E-02

```

1  TITLE DRSPALL SENSITIVITY SAMPLING
0  HISTOGRAM FOR VARIABLE NO. 3  LOGUNIFORM  DISTRIBUTION
    
```

MIDPOINT	FREQ.	
0.3699998E-13	10	XXXXXXXXXX
0.1109999E-12	4	XXXX
0.1849999E-12	2	XX
0.2589999E-12	3	XXX
0.3329998E-12	1	X
0.4069998E-12	1	X
0.4809997E-12	1	X
0.5549997E-12	1	X
0.6289996E-12	0	
0.7029996E-12	1	X
0.7769995E-12	1	X
0.8509994E-12	1	X
0.9249994E-12	0	
0.9989994E-12	0	
0.1072999E-11	1	X
0.1146999E-11	0	
0.1220999E-11	1	X
0.1294999E-11	1	X
0.1368999E-11	0	
0.1442999E-11	0	
0.1516999E-11	1	X
0	30	

MIN	MAX	RANGE	MEAN	MEDIAN	VARIANCE
-----	-----	-------	------	--------	----------

0.1763018E-13 0.1498357E-11 0.1480727E-11 0.3667784E-12 0.1643786E-12 0.1769211E-24

1 TITLE DRSPALL SENSITIVITY SAMPLING  
 0 HISTOGRAM FOR VARIABLE NO. 4 UNIFORM DISTRIBUTION

MIDPOINT	FREQ.	
0.3529499	2	XX
0.3568499	1	X
0.3607499	2	XX
0.3646499	2	XX
0.3685499	1	X
0.3724499	1	X
0.3763499	1	X
0.3802499	2	XX
0.3841498	2	XX
0.3880498	1	X
0.3919498	2	XX
0.3958498	1	X
0.3997498	1	X
0.4036498	2	XX
0.4075498	1	X
0.4114498	2	XX
0.4153498	1	X
0.4192498	1	X
0.4231498	2	XX
0.4270498	1	X
0.4309497	1	X
0	30	

MIN	MAX	RANGE	MEAN	MEDIAN	VARIANCE
0.3512448	0.4293006	0.7805583E-01	0.3900402	0.3894181	0.5430857E-03

1 TITLE DRSPALL SENSITIVITY SAMPLING  
 0 HISTOGRAM FOR VARIABLE NO. 5 LOGUNIFORM DISTRIBUTION

MIDPOINT	FREQ.	
121200.0	2	XX
123600.0	2	XX
126000.0	1	X
128400.0	2	XX
130800.0	1	X
133200.0	2	XX
135600.0	2	XX

138000.0	0	
140400.0	2	XX
142800.0	2	XX
145200.0	1	X
147600.0	2	XX
150000.0	1	X
152400.0	1	X
154800.0	2	XX
157200.0	0	
159600.0	2	XX
162000.0	2	XX
164400.0	1	X
166800.0	1	X
169200.0	1	X
0	30	

MIN	MAX	RANGE	MEAN	MEDIAN	VARIANCE
120370.0	168878.5	48508.51	143374.6	142759.0	0.2096278E+09

1 TITLE DRSPALL SENSITIVITY SAMPLING  
 0 HISTOGRAM FOR VARIABLE NO. 6 UNIFORM DISTRIBUTION

MIDPOINT	FREQ.	
1149.500	2	XX
1160.500	1	X
1171.500	2	XX
1182.500	1	X
1193.500	2	XX
1204.500	1	X
1215.500	1	X
1226.500	1	X
1237.500	2	XX
1248.500	1	X
1259.500	2	XX
1270.500	1	X
1281.500	1	X
1292.500	1	X
1303.500	2	XX
1314.500	2	XX
1325.500	1	X
1336.500	1	X
1347.500	2	XX
1358.500	1	X
1369.500	2	XX

0 30

MIN	MAX	RANGE	MEAN	MEDIAN	VARIANCE
1147.682	1372.191	224.5092	1259.770	1259.989	4754.800

1 TITLE DRSPALL SENSITIVITY SAMPLING

0 HISTOGRAM FOR VARIABLE NO. 7 UNIFORM DISTRIBUTION

MIDPOINT	FREQ.
----------	-------

0.5399999E-02	1	X
0.6599999E-02	2	XX
0.7799999E-02	1	X
0.8999999E-02	1	X
0.1020000E-01	2	XX
0.1140000E-01	1	X
0.1260000E-01	2	XX
0.1380000E-01	1	X
0.1500000E-01	2	XX
0.1620000E-01	1	X
0.1740000E-01	1	X
0.1860000E-01	2	XX
0.1980000E-01	1	X
0.2100000E-01	2	XX
0.2220000E-01	1	X
0.2340000E-01	2	XX
0.2460000E-01	1	X
0.2580000E-01	2	XX
0.2700000E-01	1	X
0.2820000E-01	2	XX
0.2940000E-01	1	X

0 30

MIN	MAX	RANGE	MEAN	MEDIAN	VARIANCE
0.5230680E-02	0.2965956E-01	0.2442888E-01	0.1758024E-01	0.1781625E-01	0.5233707E-04

1 TITLE DRSPALL SENSITIVITY SAMPLING

0 HISTOGRAM FOR VARIABLE NO. 8 UNIFORM DISTRIBUTION

MIDPOINT	FREQ.
----------	-------

0.5916002	1	X
0.5940002	2	XX

0.5964001	2	XX
0.5988001	1	X
0.6012001	2	XX
0.6036001	1	X
0.6060001	1	X
0.6084000	1	X
0.6108000	2	XX
0.6132000	2	XX
0.6156000	1	X
0.6180000	2	XX
0.6204000	1	X
0.6227999	1	X
0.6251999	1	X
0.6275999	2	XX
0.6299999	2	XX
0.6323999	1	X
0.6347998	1	X
0.6371998	2	XX
0.6395998	1	X
0	30	

MIN	MAX	RANGE	MEAN	MEDIAN	VARIANCE
0.5908749	0.6398594	0.4898453E-01	0.6150166	0.6150127	0.2086004E-03

1 TITLE DRSPALL SENSITIVITY SAMPLING  
 0 HISTOGRAM FOR VARIABLE NO. 9 UNIFORM DISTRIBUTION

MIDPOINT	FREQ.
-1.783500	2 XX
-1.754500	1 X
-1.725500	2 XX
-1.696500	1 X
-1.667500	2 XX
-1.638500	1 X
-1.609500	1 X
-1.580500	2 XX
-1.551500	2 XX
-1.522500	1 X
-1.493500	1 X
-1.464500	1 X
-1.435500	2 XX
-1.406500	1 X
-1.377500	2 XX
-1.348500	1 X

```

-1.319499      2   XX
-1.290499      1   X
-1.261499      2   XX
-1.232499      1   X
-1.203499      1   X
0              30
    
```

MIN	MAX	RANGE	MEAN	MEDIAN	VARIANCE
-1.787823	-1.208417	0.5794060	-1.499879	-1.501855	0.3027242E-01

```

1  TITLE DRSPALL SENSITIVITY SAMPLING
0  HISTOGRAM FOR VARIABLE NO. 10   UNIFORM   DISTRIBUTION
    
```

MIDPOINT	FREQ.
0.3010000E-02	2 XX
0.3150000E-02	1 X
0.3290000E-02	1 X
0.3430000E-02	1 X
0.3570000E-02	2 XX
0.3710000E-02	1 X
0.3850000E-02	2 XX
0.3990000E-02	1 X
0.4130000E-02	2 XX
0.4270000E-02	1 X
0.4410000E-02	1 X
0.4550000E-02	2 XX
0.4690000E-02	1 X
0.4830000E-02	2 XX
0.4970001E-02	1 X
0.5110001E-02	2 XX
0.5250001E-02	1 X
0.5390001E-02	1 X
0.5530001E-02	1 X
0.5670001E-02	2 XX
0.5810001E-02	2 XX
0	30

MIN	MAX	RANGE	MEAN	MEDIAN	VARIANCE
0.3012818E-02	0.5838518E-02	0.2825700E-02	0.4433378E-02	0.4444232E-02	0.7353703E-06

```

1  TITLE DRSPALL SENSITIVITY SAMPLING
0  HISTOGRAM FOR VARIABLE NO. 11   UNIFORM   DISTRIBUTION
    
```

MIDPOINT	FREQ.
0.1618500E-01	1 X
0.1657500E-01	2 XX
0.1696500E-01	1 X
0.1735500E-01	1 X
0.1774500E-01	2 XX
0.1813500E-01	1 X
0.1852500E-01	1 X
0.1891500E-01	3 XXX
0.1930500E-01	1 X
0.1969500E-01	1 X
0.2008501E-01	1 X
0.2047501E-01	2 XX
0.2086501E-01	1 X
0.2125501E-01	2 XX
0.2164501E-01	1 X
0.2203501E-01	2 XX
0.2242501E-01	1 X
0.2281501E-01	1 X
0.2320501E-01	2 XX
0.2359501E-01	1 X
0.2398501E-01	1 X
0.2437501E-01	1 X
0	30

MIN	MAX	RANGE	MEAN	MEDIAN	VARIANCE
0.1633179E-01	0.2419202E-01	0.7860230E-02	0.2017193E-01	0.2015741E-01	0.5583186E-05

1 TITLE DRSPALL SENSITIVITY SAMPLING  
 0 HISTOGRAM FOR VARIABLE NO. 12 LOGUNIFORM DISTRIBUTION

MIDPOINT	FREQ.
0.2149999E-14	10 XXXXXXXXXXXX
0.6449998E-14	4 XXXX
0.1075000E-13	2 XX
0.1505000E-13	3 XXX
0.1935000E-13	1 X
0.2364999E-13	1 X
0.2794999E-13	1 X
0.3224999E-13	1 X
0.3654999E-13	0
0.4084999E-13	2 XX

```

0.4514999E-13      0
0.4944999E-13      1   X
0.5374999E-13      0
0.5804999E-13      1   X
0.6234999E-13      0
0.6664999E-13      1   X
0.7094999E-13      0
0.7524999E-13      1   X
0.7954999E-13      0
0.8384999E-13      0
0.8814999E-13      1   X
0
30
    
```

MIN	MAX	RANGE	MEAN	MEDIAN	VARIANCE
0.1036870E-14	0.8671365E-13	0.8567678E-13	0.2114528E-13	0.1018933E-13	0.5792042E-27

```

1  TITLE DRSPALL SENSITIVITY SAMPLING
0  HISTOGRAM FOR VARIABLE NO. 13      LOGUNIFORM      DISTRIBUTION
    
```

MIDPOINT	FREQ.	
0.7500000E-04	8	XXXXXXXX
0.2250000E-03	6	XXXXXX
0.3750000E-03	2	XX
0.5250000E-03	3	XXX
0.6750001E-03	1	X
0.8250001E-03	1	X
0.9750001E-03	1	X
0.1125000E-02	2	XX
0.1275000E-02	0	
0.1425000E-02	0	
0.1575000E-02	2	XX
0.1725000E-02	0	
0.1875000E-02	0	
0.2025000E-02	1	X
0.2175000E-02	1	X
0.2325000E-02	0	
0.2475000E-02	0	
0.2625000E-02	1	X
0.2775000E-02	0	
0.2925000E-02	0	
0.3075000E-02	1	X
0	30	

MIN	MAX	RANGE	MEAN	MEDIAN	VARIANCE
0.5510329E-04	0.3087521E-02	0.3032418E-02	0.7382859E-03	0.3964929E-03	0.6506905E-06

1 TITLE DRSPALL SENSITIVITY SAMPLING  
 0 HISTOGRAM FOR VARIABLE NO. 14 UNIFORM DISTRIBUTION

MIDPOINT	FREQ.
0.1100000	1 X
0.1540000	2 XX
0.1979999	1 X
0.2419999	1 X
0.2859999	2 XX
0.3299999	1 X
0.3739999	2 XX
0.4179999	2 XX
0.4619999	1 X
0.5059999	1 X
0.5499999	1 X
0.5939999	2 XX
0.6379998	2 XX
0.6819998	1 X
0.7259998	2 XX
0.7699997	1 X
0.8139997	1 X
0.8579997	2 XX
0.9019997	1 X
0.9459996	2 XX
0.9899996	1 X
0	30

MIN	MAX	RANGE	MEAN	MEDIAN	VARIANCE
0.1076704	0.9945842	0.8869138	0.5501117	0.5542962	0.6719758E-01

1 TITLE DRSPALL SENSITIVITY SAMPLING  
 0 HISTOGRAM FOR VARIABLE NO. 15 UNIFORM DISTRIBUTION

MIDPOINT	FREQ.
0.1075000E-02	1 X
0.1505000E-02	1 X
0.1935000E-02	2 XX
0.2365000E-02	1 X
0.2795000E-02	2 XX

```

0.3225000E-02      1      X
0.3655000E-02      1      X
0.4085000E-02      2     XX
0.4515000E-02      2     XX
0.4945000E-02      1      X
0.5375000E-02      1      X
0.5805000E-02      2     XX
0.6235000E-02      1      X
0.6665000E-02      1      X
0.7095000E-02      2     XX
0.7525000E-02      1      X
0.7955000E-02      2     XX
0.8385000E-02      1      X
0.8815000E-02      2     XX
0.9245000E-02      1      X
0.9675000E-02      2     XX
0
30
    
```

```

MIN          MAX          RANGE          MEAN          MEDIAN          VARIANCE
0.1055460E-02  0.9714357E-02  0.8658896E-02  0.5495924E-02  0.5439280E-02  0.6745872E-05
    
```

```

1TITLE DRSPALL SENSITIVITY SAMPLING
0CORRELATIONS AMONG INPUT VARIABLES CREATED BY THE LATIN HYPERCUBE SAMPLE FOR RAW DATA
0      1      1.0000
0      2      0.0180      1.0000
0      3      0.0738      0.0326      1.0000
0      4      0.0009      -0.0589      -0.0327      1.0000
0      5      0.0021      0.0150      0.0760      0.0276      1.0000
0      6      -0.0450      -0.0143      -0.1909      0.0054      -0.0192      1.0000
0      7      -0.0348      0.0319      0.1273      -0.0256      -0.0098      -0.0457      1.0000
0      8      -0.0439      -0.0367      -0.0743      -0.0713      -0.0324      -0.0734      0.0098      1.0000
0      9      -0.0052      0.0813      -0.1153      0.0964      0.0065      0.0240      -0.0022      0.0174      1.0000
0     10      0.0131      0.0318      -0.2082      -0.0222      0.0041      0.0044      0.0088      0.0035      0.0905      1.0000
0     11      0.0355      -0.0561      -0.0134      0.0820      -0.0182      0.0718      0.0019      0.0107      0.0315      -0.0255      1.0000
0     12      0.0702      -0.0043      -0.1006      0.0540      -0.0103      0.0917      0.0463      0.1278      0.1064      0.0464      -0.0552      1.0000
0     13      -0.0840      0.0071      -0.1197      -0.0357      -0.0773      0.0518      -0.0279      0.1005      -0.0281      -0.0854      -0.0856      0.0727      1.0000
0     14      0.0051      -0.0623      -0.0576      0.0007      0.0136      0.0300      -0.0332      -0.0052      0.0188      -0.0186      0.1821      0.0580      -0.1174      1.0000
0     15      0.0812      0.0587      -0.0229      0.0206      -0.0345      -0.0432      -0.0312      0.0599      0.0403      0.0056      -0.0053      0.1142      -0.0439      0.0002      1.0000
0      1      2      3      4      5      6      7      8      9      10      11      12      13      14      15
OVARIABLES
0THE VARIANCE INFLATION FACTOR FOR THIS MATRIX IS 1.16
1TITLE DRSPALL SENSITIVITY SAMPLING
0CORRELATIONS AMONG INPUT VARIABLES CREATED BY THE LATIN HYPERCUBE SAMPLE FOR RANK DATA
0      1      1.0000
0      2      0.0131      1.0000
    
```



## APPENDIX VARIABLE GLOSSARY

Glossary of DRSPALL variable names  
Spallings Model Peer Review  
July 7-12, 20003

*Table VG-1. Property Names*

<b>Property Name</b>	<b>Drspall input parameter</b>
SURFELEV	Land elevation
REPOSTOP	Repository top
REPOSTCK	Total thickness
DRZTCK	DRZ(disturbed Rock Zone) thickness
DRZPERM	DRZ permeability
REPOTRAD	Outer radius
REPIPRES	Initial gas pressure
FFPORPRS	Far-field Pore Pressure and Initial repository pressure
FFSTRESS	Far-field In-Situ Stress
REPIPOR	Repository initial porosity
REPIPERM	Repository initial permeability
BIOTBETA	Biot beta
PIOSRAT	Poisson's ratio
COHESION	Cohesion
FRICTANG	Friction angle
TENSLSTR	Tensile strength
PARTDIAM	Particle diameter
GASBSDEN	Gas base density
GASVISCO	Gas viscosity
INITMDEN	Initial mud density
MUDVISCO	Mud viscosity
WALLROUG	Wall roughness
MUDSOLMX	Max mud solids volume fraction
MUDSOLVE	Mud solids viscosity exponent
BITDIAM	Bit diameter
PIPEDIAM	Pipe diameter
COLRDIAM	Collar diameter
PIPEID	Pipe inside diameter
COLRLNGT	Collar length
EXITLEN	Exit pipe length
EXITDIA	Exit pipe diameter
DRILRATE	Drilling rate
INITBAR	Initial bit distance above repository

MUDPRATE	Mud pump rate
MAXPUMPP	Maximum allowed mud pump pressure
DDZTHICK	DDZ (Drill Damage Zone) thickness
DDZPERM	DDZ permeability
SDEVVR	Stop drilling exit volume rate
SPEVR	Stop pumping exit volume rate
SDTIME	Stop drilling time
MAXTIME	Max run time
PI	Pi
REFPRES	Atmospheric pressure
GRAVACC	Gravity
RGAS	Gas constant
TREPO	Repository temperature
GASDENS0	Gas base density
COMPRES	Water compressibility
RHOS	Waste density
SALTDENS	Salt density
SHAPFAC	Shape factor
TENSVEL	Tensile velocity
BITNZNO	Bit nozzle number
BITNZDIA	Bit nozzle diameter
CHOKEFF	Choke efficiency
CAVRAD0	Initial cavity radius

*Table VG-2. History Variables  
(at a location or spatial integrated value)*

<b>History Variable Name</b>	<b>Description</b>
PUMPRS	Pump pressure
BOTPRS	Well bottomhole pressure
CAVPRS	Cavity pressure
DRILLRAD	Drilled Radius (Geometry dependent Equivalent)
CAVRAD	Cavity Radius (Geometry dependent Equivalent)
TENSRAD	Tensile Radius (Geometry dependent Equivalent)
CUTRAD	Maximum Cuttings Radius (Geometry dependent Equivalent)
WBSUPVEL	Waste boundary superficial (Darcy) pore velocity
FLUIDVEL	Critical fluidization velocity
MUDEJVEL	Mud ejection velocity
WASWELL	Mass of Waste in Well
WASEJCT	Mass of Waste Ejected
CUTMASMX	Maximum possible Cuttings Mass
GASINJ	Mass of Gas Injected
WELLGAS	Mass of Gas in Well
GASEJCT	Mass of Gas Ejected
GASPOSN	Gas Position in Well
WASPOSN	Waste Position in Well
CPUTIME	CPU time
RUNSTEP	Run step Index
VOLSTORE	Volume of Waste in Storage (failed and fluidized but waiting release to wellbore)
GASTORE	Mass of Gas in Storage
WASTORE	Mass of Waste in Storage
WASINJ	Waste Injected into wellbore
GASCAV	Mass of gas in psuedo-cavity prior to penetration
SWELLGAS	Sum gas mass in each wellbore computational cell
SREPOGAS	Sum gas mass in each repository cell
GASTOTAL	Total gas in system
GASFROMW	Total gas from waste
CUTMASS	Mass of cuttings
SPLMASS	Mass of spalled material
TOTMASS	Mass of spalled and drilled waste
CUTVOLEQ	Cutting volume assuming uncompacted waste porosity=0.85
SPLVOLEQ	Spall volume assuming uncompacted waste porosity=0.85
TOTVOLEQ	Spall and drilled volume assuming uncompacted waste porosity=0.85
CUTRUVOL	True cuttings volume assuming uncompacted waste porosity=0.85 (no geometric equivalence)
CUTRUMAS	True cuttings mass (no geometric equivalence)

PUMPRATE	Mud pump rate
SHEARRAD	Maximum radius at which shear stress exceeded maximum
NOZLEVEL	Bit nozzle (Choke) fluid velocity
WBUPVEL	Wellbore velocity at well bottom
FLUIDTIM	Fluidization time for first Intact cell
SWELLGAS	Summation of gas mass in each cell
WASFROMR	Mass of waste lost from repository due to drilling and spall
WASTOTAL	Total spalled and drilled waste in system
PITGAIN	Pit gain
MUDEJCT	Mass of mud ejected

*TableVG- 3. Element Variables  
(space and time dependent)*

<b>Element Variable Name</b>	<b>Where Variable Defined</b>	<b>Description</b>
POREPRS	Repository	Repository pressure
RADEFSTR	Repository	Radial effective stress
TANEFSTR	Repository	Tangential effective stress
POREVEL	Repository	Pore velocity
RADELSTR	Repository	Radial elastic stress
TANELSTR	Repository	Tangential elastic stress
RADSPSTR	Repository	Radial seepage stress
TANSPSTR	Repository	Tangential seepage stress
FLUDSTRT	Repository	Fluidization start time
FLUDSTOP	Repository	Fluidization stop time
FAILSTRT	Repository	Failure start time
SUPRVEL	Repository	Superficial fluid velocity
FORCHRAT	Repository	Monitoring variable for Forchheimer assumption
WELLPRS	Wellbore	Well pressure
WELLVEL	Wellbore	Well velocity
WELLGSMS	Wellbore	Well gas Mass
WELLWSMS	Wellbore	Well waste Mass
WELLRHO	Wellbore	Well fluid density
WELLWSVF	Wellbore	Well waste volume fraction
WELLGSVF	Wellbore	Well gas volume fraction
WELLSAVF	Wellbore	Well salt volume fraction
WELLWSMF	Wellbore	Well waste mass fraction
WELLGSMF	Wellbore	Well gas mass fraction
WELLMDMF	Wellbore	Well mud mass fraction
WELLVOL	Wellbore	Well cell volume
COORD	Wellbore	Well cell center coordinate